

INSTITUT FOR BÆRENDE KONSTRUKTIONER OG MATERIALER

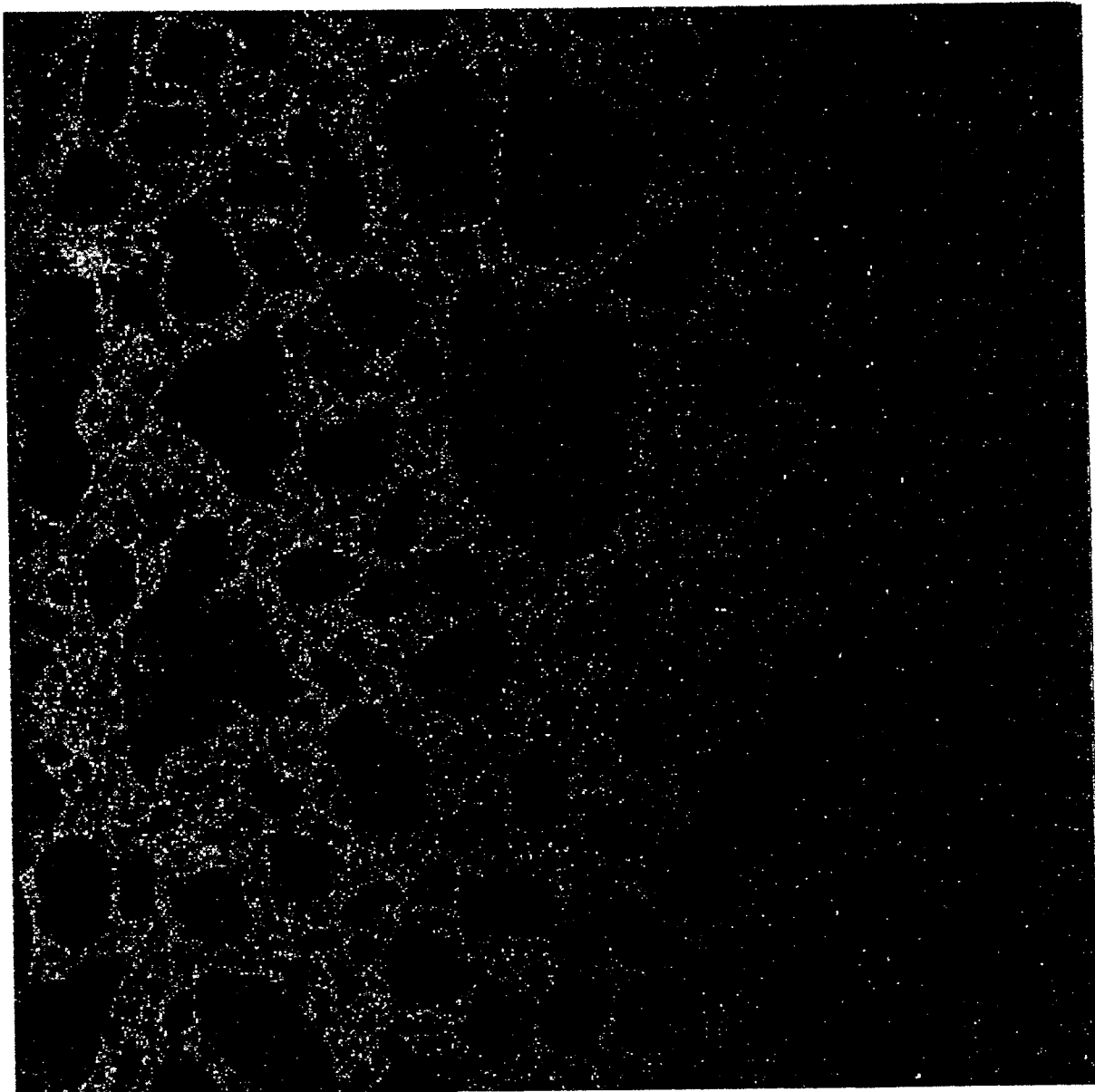


Chloride ingress in cement paste and mortar measured by Electron Probe Micro Analysis

OLE MEJLHEDE JENSEN

DEPARTMENT OF STRUCTURAL ENGINEERING AND MATERIALS
TECHNICAL UNIVERSITY OF DENMARK Series R No 51 1999

Chloride ingress in cement paste and mortar measured by Electron Probe Micro Analysis



Ole Mejlhede Jensen
December 1998

**Chloride ingress in cement paste
and mortar measured by
Electron Probe Micro Analysis**

Tryk: DTU-tryk

Danmarks Tekniske Universitet

Lyngby

ISBN 87-7740-251-0

ISSN 1396-2167

Bogbinder:

H. Meyer

FOREWORD

This report describes measurements of chloride ingress in cement paste and mortar. The measurements have been performed with a special technique: Electron Probe Micro Analysis, EPMA. The project was initiated during my stay at the University of Aberdeen in 1994-1995.

The project is carried out in cooperation with professor Fred P. Glasser and Dr. Alison Coats in the University of Aberdeen. The sample preparation and supplementary measurements have been performed at the Technical University of Denmark. The EPMA measurements have been performed by Dr. Alison Coats at the EPMA facilities in the Department of Chemistry at University of Aberdeen. Most of the subjects treated in this report have been subjected to discussions with Professor Per Freiesleben Hansen in the University of Aalborg. Dr. Lauge Fuglsang Nielsen in the Technical University of Denmark has helped with the composite modelling. Dr. Anders Nielsen and Dr. Kurt Kielsgaard Hansen both of the Technical University of Denmark are thanked for their kind help and support during the project.

A number of facilities have been used at different departments of the Technical University of Denmark:

Dr. Rolf W. Berg at the Department of Chemistry helped with determination of sodium concentration, *Héctor Diaz* at the Department of Geology and Geotechnical Engineering helped with diamond cutting, *Dr. Susanne Jacobsen* at the Department of Biochemistry and Nutrition helped with freeze drying, and *Annemarie Ripa* at the Department of Manufacturing Engineering helped with the pH measurements.

The help from all these persons is hereby greatly acknowledged.

The project was made possible thanks to a grant from the Danish Council for Technical Scientific Research.

Front cover picture: Electron Probe Micro Analysis map of chloride in a cement mortar with a water-cement ratio of 0.3. The mortar has been exposed to a 3% NaCl solution for 3 months. The chloride exposed surface is to the left. The area shown is approximately 1 by 1 cm.

CONTENTS

Foreword	1
Contents	
1 Introduction	3
2 Experimental	4
2.1 Summary of experiments	4
2.2 Experimental schedule	5
2.3 Materials	5
2.4 Mixing, pouring and curing	6
2.5 Initial capillary saturation and grinding	6
2.6 Polyurethan coating	7
2.7 Capillary saturation	7
2.8 Chloride exposure	7
2.9 Cutting	9
2.10 Drying	9
2.11 Degree of hydration	9
2.12 Embedding in epoxy	9
2.13 Polishing	10
2.14 EPMA measurements	11
2.15 Traditional chloride profile measurements	12
3 Results and discussion	13
3.1 Control of exposure liquid and degree of hydration	13
3.2 Leaching	13
3.3 Influence of superplasticizer	14
3.4 Influence of mixing on chloride profile fluctuations	15
3.5 EPMA compared with traditional profile measurements	16
3.6 Influence of aggregate	17
3.7 Influence of water-cement ratio	20
3.8 Influence of silica fume	21
3.9 Influence of temperature	22
3.10 Influence of exposure time	23
4 Modelling	25
4.1 Computer program for ingress modelling	25
4.2 Calculated diffusion coefficients	27
4.3 Composite theory	30
5 Conclusion	34
5.1 Further research	34
Appendix A	35
Appendix B	36
Appendix C	39
Appendix D	41
Appendix E	43
Appendix F	49
Appendix G	50
Appendix H	52
Literature	59

1 INTRODUCTION

Chloride ingress is a common cause of deterioration of reinforced concrete structures. Concrete may be exposed to chloride by sea water or deicing salts. The chloride initiates corrosion of the reinforcement which through expansion disrupts the concrete. In addition, the corrosion reduces the cross section of the reinforcement.

Modelling the chloride ingress is an important basis for designing the durability of concrete structures. As an example the Danish Great Belt link is designed to have 100 years durability based on calculation of chloride ingress¹⁸. During the last 15 years the types of concrete used in practice have changed substantially. Due to plasticizers and mineral additives concretes with higher strengths and reduced permeability are produced. Recently it has become clear that traditional chloride ingress models do not apply to modern concretes. Actually, the life time model used for the Danish Great Belt link has shown up to be based on wrong assumptions¹⁸.

Ficks law of diffusion has been the basis of chloride ingress modelling since 1970. However, especially for modern concretes such a chloride ingress model lacks physical substance; At best it may only serve as a pure mathematical model.

Chloride ingress in modern concretes cannot be followed with conventional measuring techniques. This makes it difficult to develop and test new models. However, prefatory experiments have shown that electron probe micro analysis, EPMA, is applicable for this purpose¹⁹. The geometric resolution for the EPMA method is 100-1000 times better than for conventional techniques.

The present project is aimed to give a better understanding of the physico-chemical nature of chloride ingress. A number of different cement pastes and mortars are examined ranging from traditional to modern high-performance types. The pastes and mortars are exposed to synthetic seawater from 1 day to half a year. Thereafter, the samples are examined by EPMA.

Modelling of the measured profiles focuses on a physico-chemical understanding of the mechanisms.

2 EXPERIMENTAL

2.1 SUMMARY OF EXPERIMENTS

Table 1 shows a summary of the pastes and mortars examined.

Type	w/c	% s.f.	SPC	Chloride exposure time (days)						
				1	3	7	14	30	90	180
Paste	0.2	0	+					#9		
	0.3	0	+	#1	#3	#5	#7	#10	#28	#32
		3	+					#11		
		6	+					#12		
		10	+					#13		
		20	+	#2	#4	#6	#8	#14	#29	#33
	0.4	0	÷					#15		
	0.5	0	+					#16		
		3	+					#17		
		6	+					#18		
	0.5	0	÷					#19		
		3	÷					#20		
		6	÷					#21		
		10	÷					#22		
		20	÷					#23		
	0.6	0	÷					#24		
	0.7	0	÷					#25		
Mortar	0.3	0	+					#26	#30	
		20	+					#27	#31	

Table 1. Composition of pastes and mortars examined. A number is given for each sample. Addition of superplasticizer (SPC) to the mixtures is marked by "+". The water-cement ratio is the pure weight ratio of water to cement. The silica fume percentage is the weight ratio of silica fume to cement. All samples were exposed to a 3% NaCl solution as described in section 2.8. In addition replicas of some of the samples were exposed to a special 3% NaCl solution which minimized leaching, c.f. section 2.8.1. The sample numbers for these samples are underlined. Anti leach samples #10 and 14 were chloride exposed at 4, 20 and 35°C. All other samples were exposed at 20°C.

The chloride ingress for all samples in Table 1 is detected with Electron Probe Micro Analysis, EPMA. In order to test the EPMA technique traditional measurements of chloride profiles are carried out on sample #14 (20°C) and #19.

For the sake of chloride ingress modelling the chloride binding properties of the cement pastes have to be known. This is examined in a M.Sc. project³ which has run parallel to the present project. Experimental results from this M.Sc. project are used in the modelling.

2.2 EXPERIMENTAL SCHEDULE

The experimental procedure generally follows the Nordic Test Method NT Build 443¹⁶. Depending on the necessary chloride exposure time the experimental schedule is as follows:

Day	Action
0	Mixing: water addition in two steps followed by evacuation Pouring of the paste into tight moulds
0→1	Rotation of the paste to avoid bleeding
1→30	Paste in moulds kept in a humidstat (=desiccator)
30	Demoulding
30→100	Water saturation in a humidstat with lime-water 1. week: Evacuated 2. week: Atmospheric pressure 1 mm of sample base is grinded off Surface drying followed by polyurethan coating (the sample base is left uncoated) 3. week: Evacuated Weighing of samples 4-8½ week: Atmospheric pressure Weighing of samples every week
100→130	Chloride exposure: each sample in a separate ¾ l jar with a 3% NaCl-solution
130	Diamond cutting of samples Control of ion concentration in exposure liquids
130-160	Vacuum drying of samples Measurement of the degree of hydration by ignition: 105-1050°C
160-170	Casting into epoxy, polishing
170	Carbon coating and EPMA measurements
200	Data processing and modelling

In the following paragraphs each of the above experimental steps are described in detail.

2.3 MATERIALS

2.3.1 Cement

Rapid-hardening white Portland cement with a Blaine fineness of 419 m²/kg was used. Bogue-calculated phase composition and other data for the cement are given in Table 2.

C ₃ S	C ₂ S	C ₃ A	C ₄ AF	CaSO ₄	Free CaO	Na ₂ O eq.	LOI
66.1	21.2	4.3	1.1	3.6	1.96	0.17	0.86

Table 2. Chemical data for the cement (wt%).

2.3.2 Silica fume

Dry silica fume with a specific surface area of 20.5 m²/g was used. The chemical composition is given in Table 3.

SiO ₂	Al ₂ O ₃	Fe ₂ O ₃	MgO	SO ₃	Na ₂ O eq.	LOI
90.76	0.54	0.94	1.32	0.57	0.59	2.45

Table 3. Chemical data for the silica fume (wt%).

2.3.3 Superplasticizer

The superplasticizer is a naphthalene based dry powder. The superplasticizer was added at a rate of 1% by weight of cement + silica fume. Superplasticizer was added at $w/c=0.2$ and 0.3 . To test the influence of superplasticizer on chloride ingress samples at $w/c=0.5$ were produced both with and without superplasticizer, cf. Table 1.

2.3.4 Sand

Standard quartz sand 0-4 mm was used for the mortars. The sand was added by volume amounting to 58% of the total mortar volume (one bag of standard sand, 1350 g per 367.9 cm³ paste).

2.3.5 Water

Demineralized, freshly boiled water was used (=de-aired).

2.4 MIXING, POURING AND CURING

The materials are approximately 20°C at mixing. The mixer is a 5 litre epicyclic standard laboratory mixer. Mixing is performed for 5 minutes at speed level two. The water is added in two steps during mixing: without superplasticizer mixing is started at $w/c=0.25$, and with superplasticizer at $w/c=0.20$. This procedure improves the homogeneity of the paste and the dispersion of the silica fume. According to light microscopy approximately 1% of the silica fume is agglomerated in the cement paste.

After mixing the paste is evacuated for 30 seconds with continuously stirring. During this process the paste will come to the boil. The moulds are filled on a vibrating table. The paste is poured from the evacuation container into the mould in a jet (as far as possible) to avoid encapsulation of air in the cement paste; Air bubbles may after water saturation "short-circuit" the chloride ingress. The moulds are circular cylindrical with a diameter of approximately 44 mm and a length of 21 mm.

The first day after mixing the cement paste is rotated to avoid bleeding. This is mainly important at high w/c ratios. Thereafter, the sealed samples are transferred to humidstats (=desiccators). The paste hardens sealed for 1 month. Hydration will roughly be completed at this time, since white portland cement is a rapid-hardening cement. Especially at low w/c ratios sealed curing is the only way to ensure a homogeneous pore structure throughout the cement paste; even by water curing a dense paste may not be water saturated. This will lead to a different pore structure in the surface zone compared to the center of the sample.

After demoulding the side of the sample is marked with a pencil. The information includes sample identification and the position of the downward side during pouring. The downward side contains the fewest air-bubbles and is the most homogeneous, and is, therefore, used as the chloride exposed surface.

2.5 INITIAL CAPILLARY SATURATION AND GRINDING

After demoulding the samples are stored in $\text{Ca}(\text{OH})_2$ saturated water in a humidstat for 2 weeks. During the first week the samples are kept under vacuum and during the second week at atmospheric pressure. When the vacuum is released the air space in the humidstat is filled with N_2 .

After this initial water saturation approximately 1 mm is grinded off the sample base which will be used as chloride exposed surface. The water grinding is performed with SiC 500 paper followed by SiC 1000. The chloride exposed surface will thus be an internal surface. This has been chosen since it is the chloride diffusion in the internal pore system which is aimed to be examined. The micro structure close to a mould or air is different from the bulk¹¹. To eliminate the influence of such a layer it is removed. Due to hardness of the mortars 1.5 mm were removed by diamond cutting followed by grinding to smoothen the cutting surface.

2.6 POLYURETHAN COATING

After grinding of the sample base the samples are placed on a plastic film (kitchen freezing bags) and exposed to the laboratory air until the surface has been dried to a stable level. After 10 hours drying an approximately 1 mm thick polyurethan coating is applied to all surfaces but the grinded base. If the surface of the cement paste is not sufficiently dried the polyurethan coating will not bind properly to the surface. The polyurethan is of the type Norco NOR 60.

According to EPMA measurements the polyurethan coating is completely chloride tight and will, therefore, restrict the chloride ingress to be one-dimensional and one-sided. If the cement paste has a sufficiently low diffusivity compared to the sample size no coating is needed. For this reason no coating was applied to the anti leach samples.

At room temperature the polyurethan will set in approximately 1 hour. After 40-45 minutes the polyurethan has become quite viscous. At that time some extra coating can be added to the sample edges, which otherwise may be difficult to cover. After approximately 9 hours the polyurethan is stick-free. Sample identification is written with permanent ink on the polyurethan.

2.7 CAPILLARY SATURATION

After 12 hours hardening of the polyurethan the samples are stored in lime saturated water under vacuum. After 1 week the surface dry weight of the samples are measured. A firmly wrung cloth is used to wipe the samples. The samples are stored for another week in lime saturated water and the surface dry weight is measured again. The samples are stored in the same liquid throughout the capillary saturation. This procedure is repeated until the weight change during a week is less than 0.1% for every sample. Thereafter, the samples are transferred to the chloride exposure jars. This criterion is more severe than the one used in the nordic test method, Nordtest¹⁶, which is 0.1% per day.

The described procedure is aimed to ensure that the samples are "completely" water-saturated - at least to an extent so that the chloride ingress is not measurably influenced by this. Air-bubbles may both block chloride ingress in certain pores as well as increase the chloride ingress into the cement paste due to capillary suction. It is intended to generate chloride diffusion in a stable, homogeneous, water saturated pore system.

The total curing time of the samples prior to chloride exposure is approximately 100 days. This ensures a stable cement system in relation to the subsequent chloride exposure time, which in most cases is 1 month. A stable cement system does not only mean that the hydration activity has leveled off but as well that potential recrystallization and the like will be relatively inactive. NMR evidence² shows that the hydration of both C_3S , C_2S and silica fume has leveled off after 100 days hardening.

During capillary saturation in lime saturated water lime deposits are observed on the surface of the samples. After the final weighing, ½ week before the capillary saturation is concluded, these deposits are grinded off with SiC 1000.

2.8 CHLORIDE EXPOSURE

The water saturated samples are exposed to a 3% NaCl-solution which approximate to the NaCl concentration in sea water. During the chloride exposure ions will leach out from the cement paste, e.g. OH^- and SO_4^{2-} . Concurrently, the chloride and sodium concentration will drop in the exposure liquid. Since the ion concentration in the exposure liquid cannot be kept constant throughout the experiment it is instead ensured that the variations during exposure are negligible.

The exposure liquids are in thermal equilibrium with the samples before use. Each sample is placed in a separate container with the exposed surface upwards. The containers are preserving jars with rubber

packings and spring locks. Each jar holds 750 ml exposure liquid. The ratio between exposed surface area and liquid volume will thus be $15/0.75=20 \text{ cm}^2/\text{l}$. According to the Nordtest metod¹⁶ this value must be between 20 and $80 \text{ cm}^2/\text{l}$. If it is assumed that no chloride binding takes place in the cement paste the NaCl concentration of the exposure liquid will change from 3% to 2.95% at full chloride ingress and $w/c=0.7$. This is insignificant. (A sample at $w/c=0.7$ and a degree of hydration of 0.8 will contain approximately 15 cm^3 pore water). The pH and chloride and sodium concentration in the exposure liquids are measured when the exposure is concluded. To minimize the change in the chloride concentration of the exposure liquid during the experiment it is desirable that the amount of exposure liquid is large. Conflicting with this the amount should be small to minimize leaching from the cement paste of OH^- , SO_4^{2-} etc. The chosen volume is a compromise.

The tightness of the jars was controlled by weighing. Within the weighing accuracy, 0.01 g, most of the jars were tight. Two leaky jars were transferred to humidstats, whereby the weight loss stopped.

2.8.1 Exposure liquids which minimize leaching

For some pastes special exposure liquids were prepared to minimize leaching during chloride exposure. These pastes have a water-cement ratio of 0.3 and silica fume additions from 0 to 20%, cf. Table 1. The exposure liquids were prepared by equilibrating crushed cement paste with a 3% NaCl solution. This was done as follows.

In addition to each cement paste sample for chloride exposure teflon moulds were filled with more than 500 g cement paste. After 1 day hardening the cement paste was pressed out of the teflon moulds and crushed in a 200 tons hydraulic press. The crushed material was sieved to a maximum particle size of 2 mm. A bundle was made of 500 g crushed cement paste wrapped in a cloth. The bundle was placed in the preserving jar and covered with approximately 450 ml 3% NaCl-solution. During filling the jars were evacuated to reduce the amount of encapsulated air.

After 3 months the bundles were removed from the jars leaving approximately 300 ml liquid. The chloride concentration in the exposure liquid is measured and the amount of exposure liquid in the jar is reduced to 250 ml. Due to chloride binding in the cement paste the chloride concentration in the liquids will be lower than corresponding to a 3% NaCl solution. Therefore, the chloride concentration was measured, and extra NaCl was added to the exposure liquid in order to increase the chloride concentration to this level.

The exposure liquid produced in this way will, apart from the NaCl, be close to equilibrium with the pore fluid of the cement paste. Leaching of the cement gel is, therefore, believed to be minimized. The effect of leaching during chloride exposure is discussed in more detail in Appendix B.

2.8.2 Control of exposure liquids

The pH and chloride and sodium concentration in the exposure liquids are measured when the exposure is concluded.

The pH is measured with a temperature adjusted pH-meter. Before measurement the pH-meter is calibrated in the alkaline range.

The chloride concentration in the exposure liquid is measured with a chloride selective electrode. Three chloride standards are prepared for this purpose: 2.5%, 3% og 3.5% NaCl in distilled water. 0.1 ml chloride standard or exposure liquid is diluted with 10 ml RCT extraction liquid, c.f. Appendix A, and measured with the electrode. The electrode voltage is measured with a separate voltmeter with 0.1 mV accuracy. The chloride concentration in the exposure liquids is calculated by interpolation between the measurements on the chloride standards.

The sodium concentration is measured by flame emission spectroscopy. The measurements are given directly in mmol/l with a relative accuracy of less than 0.5% at the concentrations examined. This extraordinary accuracy is obtained by diluting the liquids with a lithium solution, which is used during measurements as a reference. However, the dilution was performed inaccurately whereby the total measuring accuracy was decreased. Measurements of sodium concentration was only performed up to 14 days chloride exposure.

2.9 CUTTING

After removal from the exposure liquid the sample surface is wiped with a paper tissue. This was not done on the 1 and 3 days samples and resulted in a greyish-white paste surface, presumably due to precipitated NaCl from the exposure liquid. To lighten the cutting process the polyurethane coating is subsequently removed. The polyurethane is easy to remove if carved with a scalpel.

The cement paste is cut with a diamond cutting wheel immediately thereafter. During cutting ethanol is used for cooling. An approximately 4 mm thick slice is cut close to the center of the sample parallel to the direction of chloride diffusion. Each cut takes approximately 15 seconds and is 1.25 mm wide. No increase in the temperature of the sample during cutting can be noted.

After cutting the direction of chloride diffusion and sample identification is marked with a pencil on the surface opposite of the polishing surface. An ethanol based marker should not be used since it will dissolve in epoxy.

2.10 DRYING

After cutting the samples are dried. This immobilizes the chloride and is required for the EPMA measurements. The samples are vacuum dried at $p < 1$ mbar with a rotary pump. This is performed at room temperature for 1 day immediately after cutting. After vacuum drying the samples are stored with fresh silica gel for 1 week followed by one further day of evacuation.

Apart from vacuum drying two other drying techniques have been tested as well. A more thorough description of these tests is given in Appendix B. According to EPMA line scan and mapping the drying does not lead to chloride removal.

2.11 DEGREE OF HYDRATION

The degree of hydration is determined by weight loss at 105-1050°C. The degree of hydration is measured on the remaining part of the cement paste sample after cutting the EPMA sample.

The samples are crushed in a mortar to a maximum particle size of 1 mm. Approximately 5 g crushed sample is dried for at least 1 hour at 105°C and the weight loss is measured during the subsequent ignition for ½ hour at 1050°C.

2.12 EMBEDDING IN EPOXY

Before embedding in epoxy approximately 1 cm of each end of the cement paste is cut off. Only the center approximately 2.3 cm is retained because the epoxy moulds cannot hold larger samples.

As embedding material Struers Epofix is used. It is unnecessary to add Epodye which is a yellow, fluorescent contrast dye. The Epofix is easy to polish, has a low heat development and does not deform during hardening. The Epofix contains a significant amount of chloride; EPMA measurements on epoxy give a chloride signal which is approximately 4 times higher than on non-exposed cement paste (from

raw materials and background noise). Epofix which has penetrated air-bubbles or cracks in the cement paste, therefore, will lead to unwanted fluctuations on the measurements. However, as long as the Epofix does not ingress into the pores the chloride content in the Epofix is no problem.

The epoxy is poured into Ø 40 mm polypropylene moulds. The epoxy layer should at maximum be 15 mm thick for the sake of the EPMA sample holder. To minimize the subsequent sample preparation the moulds should not be filled more than this.

The cement paste is submerged into the Epofix after evacuation. This minimizes ingress of Epofix into the pores of the cement paste. The chosen polishing surface of the cement paste is facing the bottom of the mould. Air-bubbles in the epoxy, which are brought into the epoxy during submerging the cement paste, are removed. For the sake of the EPMA measurements the cement paste should be placed with at least 3 mm free space from the edge of the mould.

According to the producer the hardening time of the Epofix is 8 hours at 20°C. However, it should harden for 2 days to obtain sufficient hardness for polishing. The hardening can be accelerated by raising the temperature. After 8 hours at 20°C the samples can be stored at 40°C. In this way a total hardening time of 1 day is sufficient. Higher temperatures during hardening should not be used since it may lead to cracking of the cement paste.

2.13 POLISHING

The necessary grinding and polishing time varies greatly with the type of cement paste or mortar. The hard mortars may require a new piece of grinding paper for every sample and may need 4 times longer grinding time than the softer pastes. The times given below should, therefore, be considered as a guide.

The back of the sample is plane grinded on SiC 220 paper. The thickness of the sample should be less than 15 mm for the sake of the sample holder for the EPMA machine. To make the sample identification on the back of the cement paste readable scratches from the first grinding is removed with SiC 500, SiC 1000 and a short 3 µm diamond polishing.

From the polishing surface of the sample 0.5 mm is removed with SiC 80. This uncovers the cement paste. Furthermore, it removes the outer layer of the cement paste which potentially may contain epoxy filled pores or may be deformed or cracked by the cutting process. Thereafter, grinding is done with SiC 220. This leaves surface deformations of approximately 80 µm - the deformation depth is approximately 4 times the grain size (SiC 220 has a grain size of approximately 20 µm).

Subsequently the edge of the polishing surface of the sample is made round on SiC 220.

During all grinding and polishing steps the rotary disk is added ethanol. This cools the sample and removes off-grounded material. The sample is pressed gently against the rotary dish and circulated in a regular motion opposite the direction of rotation. This counteracts preferential scratching and promotes planeness of the sample. Ethanol is used in order not to dissolve chloride during sample preparation. The ethanol has a purity of more than 99.9%.

The planeness of the sample is controlled with a straightness gauge. The SiC 220 grinding step is repeated if the planeness is unsatisfactorily. Planeness is important since the EPMA machine focuses the electron beam assuming that the sample is plane. Furthermore, the following grinding and polishing steps are facilitated if the sample is plane. The planeness of the sample is reduced during the following grinding and polishing steps. The times suggested in the following should, therefore, not be extended unnecessarily.

The grinding is concluded with ethanol suspended SiC 1000 on a glass plate for 2 minutes at 100 rpm. SiC 1000 leaves surface deformations of 12 µm.

Between each of the above mentioned grinding steps the sample is rinsed with ethanol and wiped with a paper towel (kitchen roll). After the polishing steps Joseph paper (lens tissue) is used since paper towel may produce up to 3 μm scratches.

After the final grinding and each polishing step the sample is ultrasonic rinsed in ethanol for 1 minute. The ultrasonic rinsing ensures that no particles are transferred between the polishing steps. The sample is placed on the side during ultrasonic rinsing in order not to damage the polishing surface and to ensure that released particles leaves the polishing surface. Fresh ethanol is used for each polishing step.

Initial polishing is done with 3 μm polycrystalline diamonds for 3 minutes on a Struers Pan paper cloth (previous name: Pan-W). A slightly worn cloth functions better than a new one. A new cloth can initially be worn with the edge of a microscope slide or the back of a sample. During this process the cloth should be kept moist with ethanol. The cloth will stand for approximately 30 samples.

The diamonds are added as spray. For every sample fresh diamond spray is added for approximately 1 second. During polishing the cloth is kept moist with ethanol.

1 μm diamond polishing is done for 1 minute on another cloth of the same type. Fresh diamonds are added for every second sample. Final polishing is done with 1 μm diamonds on a NAP-cloth for 15 seconds. Adding a small amount of $\frac{1}{4}$ μm diamonds enhances lustering of the sample.

Each grinding and polishing step can be controlled with light microscope. An unsatisfactorily polishing step and possibly as well the previous step have to be repeated.

2.14 EPMA MEASUREMENTS

A Cameca SX51 EPMA instrument equipped with four wavelength dispersive spectrometers is used for the chloride profile measurements. Compared to a traditional scanning electron microscope with an energy dispersive spectrometer the measuring accuracy may be 10 times better.

An accelerating voltage of 20 kV and a beam current of 20 nA is used. At these conditions the volume of sample analyzed is roughly 1-2 μm^3 for each point. Before EPMA measurements the sample is sputter coated with a conductive carbon layer. This prevents charging of the sample under the electron beam.

The EPMA measurements are performed either as qualitative line scans or maps. A line scan has typically 1000 analyzed points. The x-ray counting time is 1 second per point. A typical EPMA line scan takes approximately 20 minutes to perform. Line scans were only performed on the pastes.

The mortars and most of the pastes were in addition analyzed by EPMA mapping. In this technique a grid of points is measured giving an element map of the sample surface. In this different mode of operation the electron beam is defocused and a short x-ray counting time is used. An element map of 512 \times 512 points takes 4 hours to perform for a time constant of 50 ms. The maps are presented either as pictures or as graphs. For the pictures the chloride content in each measuring point is represented by the colour intensity. For the graphs the chloride content in a certain depth is calculated as an average of all measurements in this depth.

The results from the qualitative measurements are given as x-ray "counts" of chlorine. This arbitrary unit is previously shown to be approximately proportional to the chloride content¹⁹.

In addition to the chloride count the EPMA measurements automatically include counts of calcium and silicon. This additional information is used for the detection of the sample edge; The first measurements of a map and a line scan are taken in the epoxy. Since the epoxy, contrary to the cement paste, does not contain calcium the sample edge is easy to identify. Besides this the calcium and silicon measurements have been used to examine leaching, c.f. Appendix B.

2.15 TRADITIONAL CHLORIDE PROFILE MEASUREMENTS

Traditional chloride profile measurements are performed with a commercial test kit, Germann's RCT test (Rapid Chloride Test). Two samples are examined: w/c=0.3, 20% silica fume and w/c=0.5, 0% silica fume after 1 month, 20°C chloride exposure (sample #14, leached, and #16 in Table 1). Slices are cut from the remaining sample parts after the EPMA samples are cut. The thickness of the slices are approximately 1.25 mm. The width of the kerf is approximately 1.25 mm. On each sample half the kerfs are displaced as to measure an intact profile. The slices are dried at 105°C followed by crushing in a mortar before the RCT test. Each crushed sample weighs approximately 1-1.5 g. The RCT test is based on a sample size of 1.5 g but the measured chloride concentration can simply be scaled at other sample sizes; at 0.75 g sample the measured value has to be doubled.

The chloride content is measured with a chloride selective electrode. This is done after extraction of chloride from the cement pastes with a special extraction liquid. The extraction liquid is described in Appendix A.

3 RESULTS AND DISCUSSION

In this section chloride ingress profiles are presented. The results are mainly discussed qualitatively; a more thorough quantitative analysis is given in the modelling section.

Only a few of the chloride profiles shown are based on line scans; the profile fluctuations are significantly reduced by the mapping technique. Unfortunately the chloride concentration measured by EPMA is only given as X-ray counts. X-ray counts cannot, generally, be converted into an absolute unit, since it depends on the composition of the cement paste and because the sensitivity of the EPMA probe changes with time. For easy comparison each profile has been scaled arbitrarily to a surface concentration of 8. Future EPMA measurements should include a chloride standard, e.g. a chloride containing cement paste in order to permit true quantitative measurements to be carried out.

Apart from Figure 5 the EPMA measurements presented in the following only show ingressed chloride; The measurements are corrected for background noise and chloride in the raw materials.³⁴

3.1 CONTROL OF EXPOSURE LIQUID AND DEGREE OF HYDRATION

Within the measuring accuracy no change in the chloride and sodium concentration of the exposure liquids is observed during exposure of the samples. Quoted as equivalent NaCl concentration both the chloride and sodium concentration has been measured to 3.0 ± 0.1 % NaCl.

Appendix F shows measuring results of exposure liquid pH and degree of hydration for the cement pastes. After exposure the pH of the exposure liquids was alkaline, typically, around 12. The measured degrees of hydration of the cement pastes are in the range 0.5-0.9, very dependent on the w/c and the silica fume content. A slight further hydration is observed during chloride exposure.

3.2 LEACHING

As mentioned in section 2.1, 2.8.1 and Appendix B, leaching during chloride exposure may significantly alter the chloride profile. Depending on the paste composition the leached zone may be 0.1-1 mm thick. The chloride profiles in the dense pastes (low w/c-ratio and silica fume addition) may be substantially changed by the leaching. This is because the leached zone is wide relative to the total chloride ingress depth. Contrary to this leaching may be considered an insignificant surface phenomenon for the pastes at a high w/c-ratio.

Figure 1 shows an example of the influence of leaching of a highly affected sample.

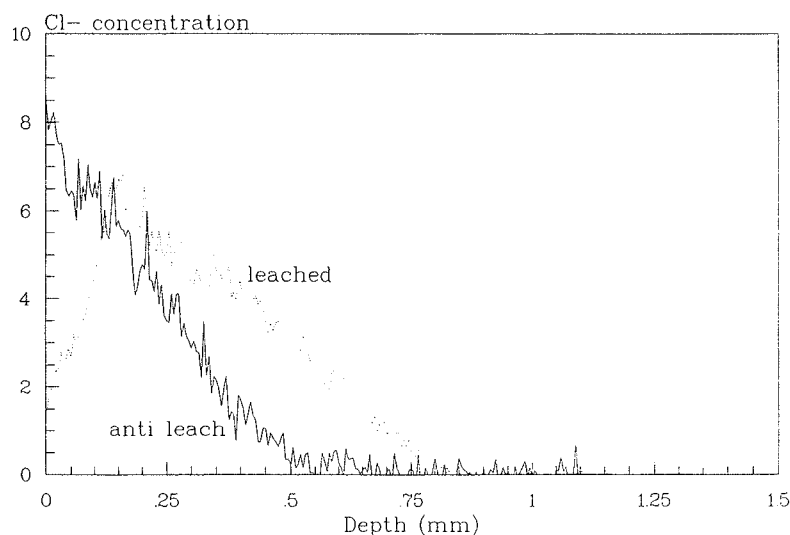


Figure 1. Influence of leaching on chloride ingress. Chloride profiles in two identical pastes are shown. Both pastes have a w/c-ratio of 0.3 with 10% silica fume addition and have been chloride exposed for 1 month. One of the pastes has been exposed to a pure 3% NaCl solution whereby leaching takes place. The other paste has been exposed to a 3% NaCl anti leach solution as described in section 2.8.1. The measurements are based on EPMA mapping.

As can be seen from Figure 1 precautions against leaching does change the chloride ingress. In the leached sample the chloride profile drops close to the exposed surface and the chloride ingress is deeper. This may have several reasons. First of all, the leaching removes solid material from the cement paste, primarily, calcium hydroxide, and then calcium from the C-S-H gel. This opens up the pore structure and reduces the chloride binding capacity of the cement paste. The drop in the chloride profile near the surface is most likely due to the reduced chloride binding capacity, c.f. Appendix B.

Another factor which may be important is the different pore solution compositions of the leached and the anti leach sample; The chloride does not diffuse alone, but has to be balanced by either co-diffusion of opposite charged ions or counter diffusion of identically charged ions.

No further examination of this phenomenon has been performed.

3.3 INFLUENCE OF SUPERPLASTICIZER

To test the influence of superplasticizer on chloride ingress samples at w/c=0.5 were produced both with and without superplasticizer, cf. Table 1. The superplasticizer may potentially affect the chloride ingress by modifying the pore structure, the chloride binding¹⁷ or other important ionic equilibria in the cement pore fluid³⁸. To enable mixing at low w/c-ratios superplasticizer has to be added. Furthermore, it is often claimed that superplasticizer is required to ensure proper dispersion of the silica fume. However, addition of superplasticizer at high w/c-ratios, e.g. 0.7, will severely increase the tendency to separation of the fresh cement paste.

Figure 2 shows comparative measurements of chloride ingress in cement pastes with and without superplasticizer. Based on these measurements there seems to be no influence of superplasticizer addition on the chloride ingress. Since the dispersion of the silica fume is believed to have a major influence on the chloride ingress, consequently, the superplasticizer does not seem to have any influence on the dispersion of the silica fume.

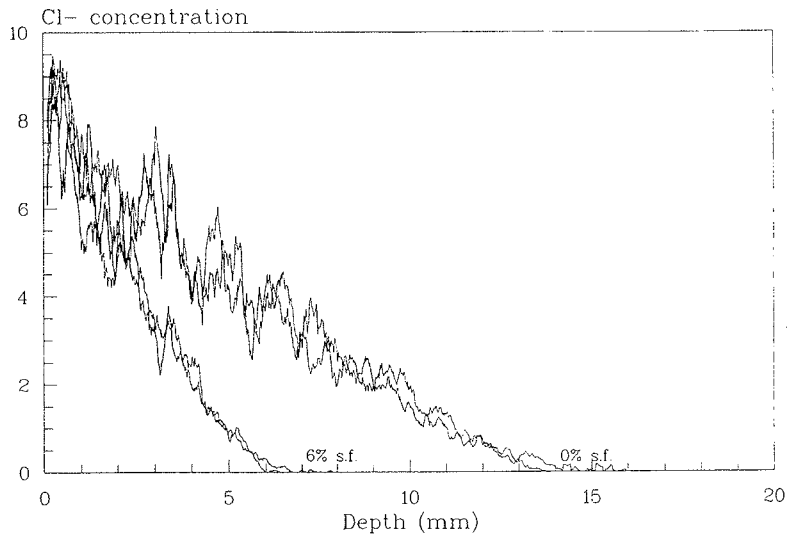


Figure 2. Influence of superplasticizer on chloride ingress. Chloride profiles in four different pastes are shown. Except from the addition of superplasticizer the pastes are identical in pairs. All the pastes have a w/c-ratio of 0.5. The curves represent 1 month chloride exposure at 0 and 6% silica fume addition. Each graph is an average of two to three line scans combined with rolling mean ± 0.1 mm around every measuring point.

3.4 INFLUENCE OF MIXING ON CHLORIDE PROFILE FLUCTUATIONS

Different types of fluctuations are observed on the EPMA chloride profiles:

1) Short-range fluctuations on a μm scale. The analyzed volume, $1\text{--}2\ \mu\text{m}^3$, may accidentally include a precipitated NaCl crystal in a pore or may include unreacted cement clinker. Therefore, fluctuations on a μm scale will inevitable exist in a cement paste. Some sort of averaging may be used to smooth the curves.

2) Long-range fluctuations on a mm scale. Presumably, this is due to local variations in the water-cement ratio. A local zone with a low water-cement ratio will have a low chloride content because it is less porous. This hypothesis was supported in a previous project¹⁹: Cement pastes with NaCl in the mix water showed mm scale fluctuations as well, even though the chloride was homogeneously distributed beforehand in the pore water¹⁹.

It is, therefore, believed that a more efficient mixing will reduce the mm scale fluctuations. Figure 3 shows chloride profiles for two cement pastes mixed in different ways. However, no major difference in mm scale fluctuations is observed between the two curves. Possibly, for the paste shown the change in mixing technique has no significant effect on local variations in water-cement ratio. At least, previous experiments have shown these two types of mixing to result in very different degrees of dispersion of the silica fume¹.

A further examination the homogeneity of cement pastes on a mm-scale should be done with mapping.

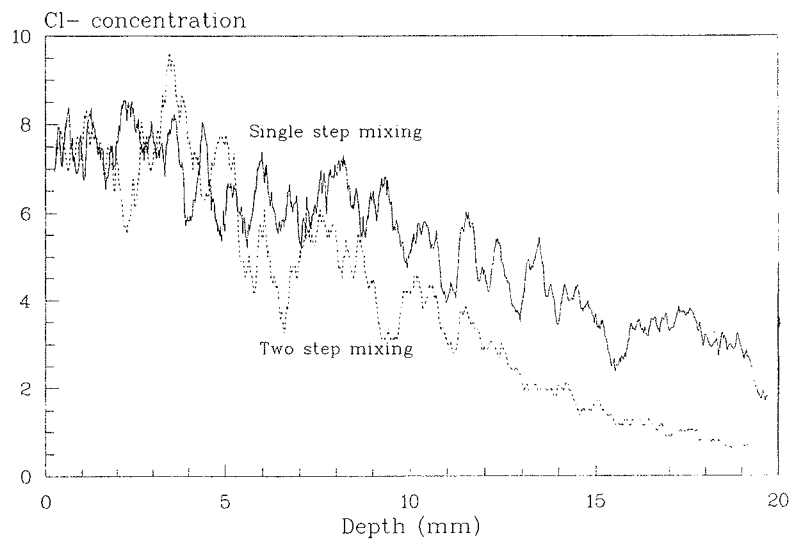


Figure 3. Comparison of mm scale fluctuations on chloride profiles. Differences in curvature and in penetration depth are due to different exposure conditions of the two pastes. Both pastes have $w/c=0.7$ but are mixed in two different ways: 1) single step mixing where the full amount of mix water is added initially, and 2) two step mixing where the cement paste initially is mixed at $w/c=0.25$. The measurements on the single step mixed paste originate from another project¹⁹. Both graphs are based on a single line scan where rolling mean ± 0.25 mm is performed around every measuring point.

3.5 EPMA COMPARED WITH TRADITIONAL PROFILE MEASUREMENTS

For comparison chloride profiles are measured in two samples both by EPMA and by the traditional method. This examination has two purposes: 1) It demonstrates the 100-1000 times higher geometric resolution of the EPMA method. This degree of resolution is required for studying high performance cement paste systems. 2) The validity of the EPMA method is checked.

Figure 4 shows chloride profiles measured by EPMA and by the traditional method.

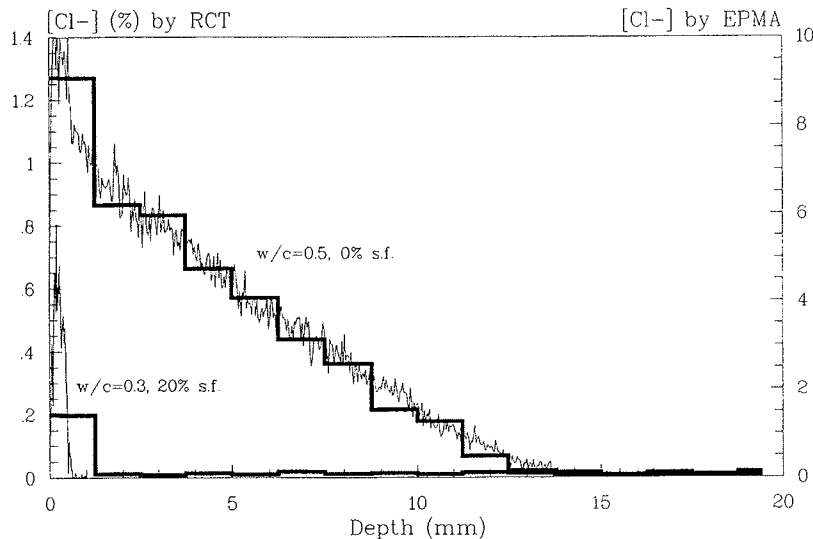


Figure 4. Comparison of chloride profiles measured by EPMA (thin line) and by the traditional method (broad line). The traditional method is performed with a commercial test kit, Rapid Chloride Test (RCT), where the chloride content is measured in 1.25 mm thick slices cut off the cement pastes. Profiles for two cement pastes are shown: 1) $w/c=0.3$ with 20% silica fume addition and 2) $w/c=0.5$ without silica fume addition. The pastes have been chloride exposure for 1 month. The EPMA graph at $w/c=0.5$ is based on mapping. The EPMA graph at $w/c=0.3$ is an average of four line scans combined with rolling mean ± 0.01 mm around every measuring point.

There are no major deviations in curvature or in chloride penetration depth between the two profiles for the $w/c=0.5$ paste. The cement paste slices for the RCT profile were cut immediately after chloride exposure, that means before drying. The coincidence of the RCT and the EPMA profile shows that no observable chloride removal takes place during EPMA sample preparation. Furthermore, it shows that the chlorine concentration given by EPMA is close to proportional to the weight percentage of chloride.

The profile for the paste at $w/c=0.3$ clearly demonstrates the geometric limitation of the traditional method. There are two reasons for this geometric limitation: 1) a macroscopic part of the cement paste is needed for the analysis and 2) samples below a certain thickness simply cannot be collected with sufficiently accuracy.

3.6 INFLUENCE OF AGGREGATE

In relation to chloride ingress some examples of important micro- and macrostructural differences between cement paste and mortar are given below:

- Mortar cannot be considered aggregate particles embedded in a homogeneous cement paste matrix. Close to the surface of the aggregate particles the cement paste is more porous compared to the bulk cement paste. This is often referred to as the paste-aggregate interfacial transition zone, ITZ, which may have a thickness³⁰ of approximately 20 μm . Relative to the bulk cement paste the ITZ has a high water-cement ratio and consequently a high diffusivity - e.g. 10 times higher³⁰. This may modify the chloride ingress.
- In a mixture with a high autogenous shrinkage the restraining effect of the aggregate particles will lead to microcracking in a mortar. Contrary, the corresponding cement paste will remain crack free if it is unrestrained. Such microcracks may act as chloride ingress routes and hence increase chloride ingress.

□ The chloride diffusivity of the aggregate particles is different from the cement paste. As an example siliceous aggregate may be impermeable to chloride ingress. In that case the chloride ingress necessarily has to follow the tortuous pathways between the aggregate particles. This will hamper the effective chloride diffusivity. Additionally, the aggregate particles dilute the cement paste, i.e. the effective sectional area is reduced. The effective chloride flux will drop due to this dilution effect.

Figure 5 shows chloride ingress at two exposure times for two cement pastes and two equivalent mortars. No difference in the chloride ingress depth between the pastes and the mortars is observed, despite the above mentioned differences between a cement paste and the equivalent mortar.

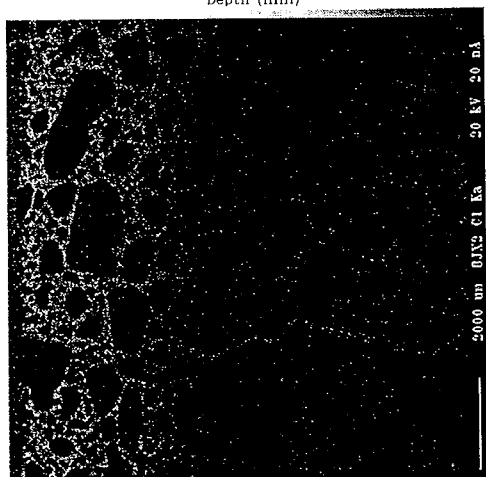
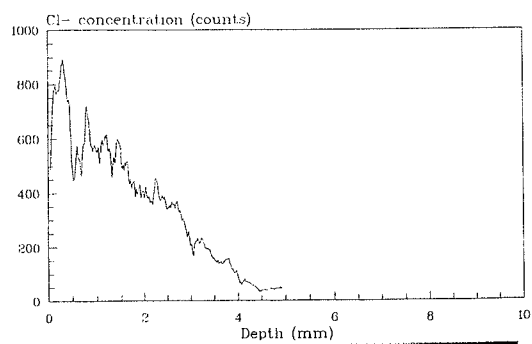
From the mortar maps it is seen that the chloride content in the quartz aggregate particles is very low. Actually, the measured chloride in the aggregate is at the detection noise level. In addition, local "shadowing" behind aggregate particles is observed. This suggests that the chloride diffusivity of the quartz particles is lower than in the cement paste. Possibly, the quartz particles are virtually impermeable. This should hamper the chloride ingress since it increases the tortuosity of the chloride ingress routes. However, there is no general difference in the chloride ingress of the mortars relative to the pastes.

Experimentally and theoretically it has been shown²³ that the silica fume containing mortar in Figure 5 will be highly microcracked, whereas the mortar without silica fume is uncracked. This is due to a very high autogenous shrinkage caused by the silica fume. Irrespective of the silica fume content both pastes are crack free because they have hardened unrestrained. However, a comparison of paste and mortar ingress shows no effect of the microcracking. This may be due to so-called autogenous healing which under moist conditions may completely block the microcracks. The healing is primarily caused by hydration of unhydrated cement which becomes exposed upon the opening of the cracks.

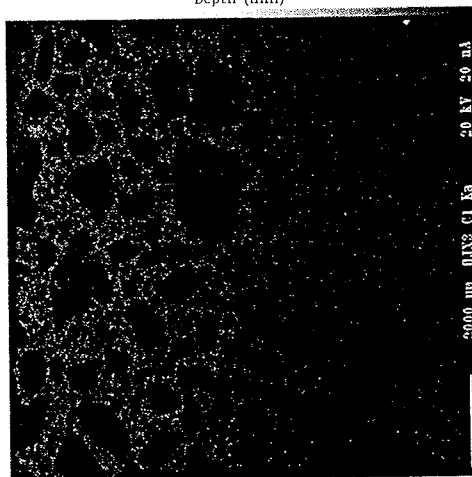
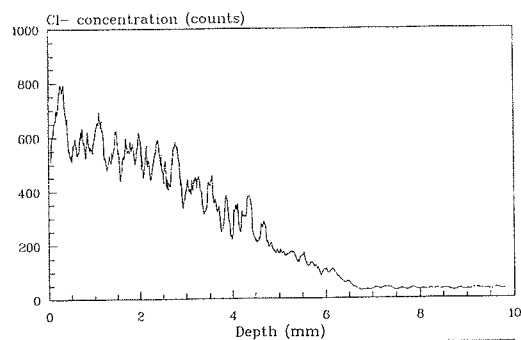
The results in Figure 5 agree with measurements in the literature³⁰; chloride diffusivity was studied in cement pastes and mortars with different sand volume fractions at water-cement ratios from 0.25 to 0.45. A further analysis of the results from this study shows that the effective chloride diffusivity is approximately proportional to the paste volume fraction. That means, the aggregate has a dilution effect on the chloride ingress, but no significant effect from ITZ and pathway tortuosity can be seen.

Figure 5. (The figure is on the next page). Comparison of chloride ingress in cement pastes and equivalent mortars. The graphs represent pastes and the maps represent mortars. The graphs are based on line scans. Each paste graph has been scaled identical to the equivalent mortar map which is just below the paste graph. Note the different geometric scaling between the four pairs. In the four uppermost diagrams the w/c-ratio is 0.3 without silica fume addition. In the four lowermost diagrams the w/c-ratio is 0.3 with 20% silica fume addition. Two exposure times, 1 month (left) and 3 months (right), are shown.

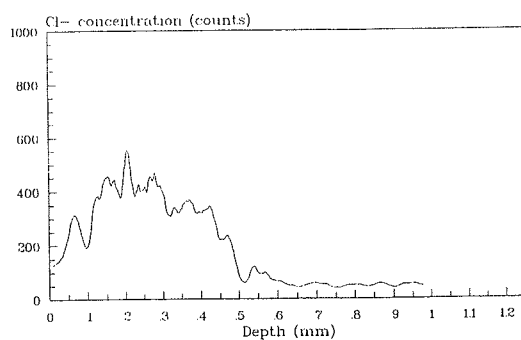
w/c=0.3, 0% s.f., 1 month



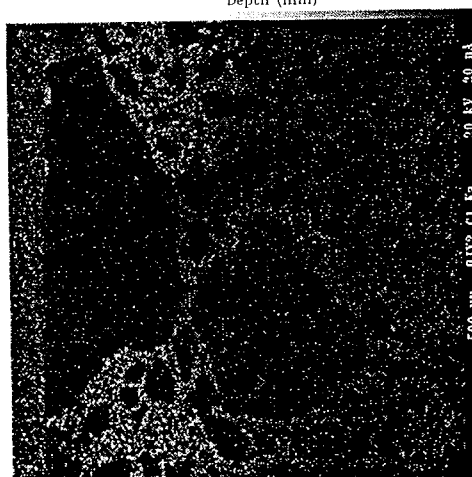
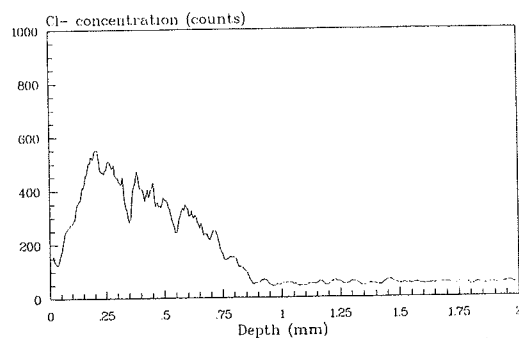
w/c=0.3, 0% s.f., 3 months



w/c=0.3, 20% s.f., 1 month



w/c=0.3, 20% s.f., 3 months



Maxwell^{27 p.186} has calculated the diffusion coefficient of a composite, D , which consists of two phases:
 1) a continuous phase and 2) periodically spaced spheres within this phase:

$$D = D_c \frac{\frac{2}{D_s} + \frac{1}{D_c} - 2\phi_s \left(\frac{1}{D_s} - \frac{1}{D_c} \right)}{\frac{2}{D_s} + \frac{1}{D_c} + \phi_s \left(\frac{1}{D_s} - \frac{1}{D_c} \right)} \quad (1)$$

Where D_c and D_s is the diffusion coefficient of the continuous phase and the spheres respectively and ϕ_s is the volume fraction of the spheres in the composite material.

If the spheres are impenetrable i.e. $D_s=0$, this equation becomes

$$D = D_c \frac{2(1-\phi_s)}{2+\phi_s} = D_c \frac{1}{1+\phi_s/2} (1-\phi_s) \quad (2)$$

At $\phi_s=0$ the factor $\frac{1}{1+\phi_s/2}$ is 1, and at $\phi_s=0.5$ the factor is 0.8. Neglecting this factor the equation is further reduced to

$$D = D_c (1-\phi_s) \quad (3)$$

This equation agrees with the above mentioned experimental observation: If the aggregate is impermeable the chloride diffusion coefficient of mortar is approximately proportional to the paste volume fraction. That means the influence of aggregate can be considered a pure dilution effect.

3.7 INFLUENCE OF WATER-CEMENT RATIO

Figure 6 shows the influence of water-cement ratio on chloride ingress. An increased water-cement ratio is seen to increase the chloride ingress. This is due to the more open and coarse pore structure at a higher water-cement ratio.

In addition the profile shape seems to depend on the water-cement ratio. At $w/c=0.2$ the profile is almost linear, whereas it tends to be more concave at higher water-cement ratios. Most likely, this phenomenon is caused by chloride binding. The lower the w/c the more chloride will be present as bound chloride relative to free chloride, see Appendix D. In the cement paste sample at $w/c=0.7$ most of the chloride is present as free chloride. The shape of the chloride profile will, therefore, mainly be controlled by Fick's law. Contrary to this, most of the chloride is present as bound chloride in the cement paste sample at $w/c=0.2$. The shape of the chloride profile will in that case be significantly modified by the chloride binding isotherm. A further account of this is given further on in the modelling section.

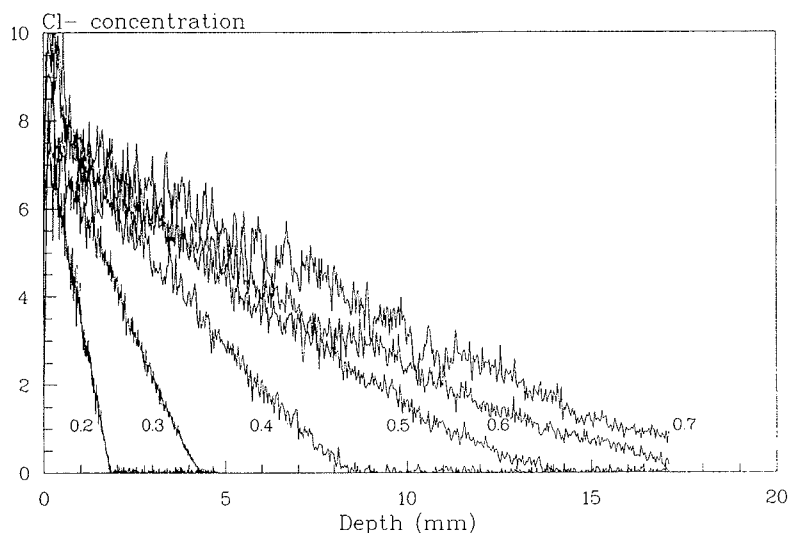


Figure 6. Influence of water-cement ratio on chloride ingress. Chloride profiles in six different pastes are shown. Except from the water-cement ratio, which is marked on the curves, the pastes are identical. The pastes do not contain silica fume and have been chloride exposed for one month. The measurements are based on EPMA mapping. The full profile at $w/c=0.6$ and 0.7 has not been measured by this technique. From line scan measurements it is known that the profile at $w/c=0.6$ levels off within the maximum depth, 20 mm. At $w/c=0.7$ the chloride has reached the bottom of the sample and is consequently accumulated.

3.8 INFLUENCE OF SILICA FUME

Figure 7 and 8 show the influence of silica fume addition on chloride ingress. Independent of the w/c -ratio, silica fume addition is seen to reduce the chloride ingress significantly. Most likely, this is due to changes in the pore structure such as pore closure and/or a finer pore structure. At least, the chloride binding is not significantly changed by silica fume addition³.

A comparison of Figure 8 and Figure 6 shows that a change in the w/c ratio from 0.5 to 0.3 roughly equals addition of 10% silica fume. This corresponds to an efficiency factor for the silica fume of 7. This is in agreement with a efficiency factor in the range 6-8 calculated by Sørensen⁴¹ from water diffusion experiments.

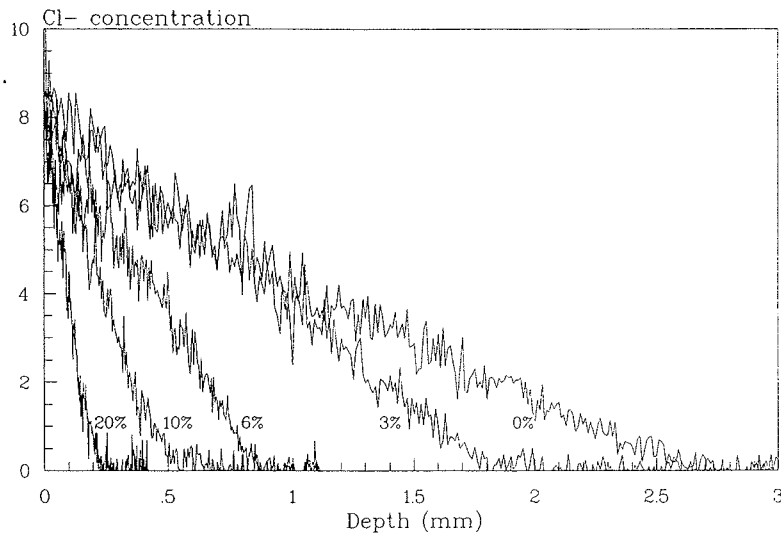


Figure 7. Influence of silica fume addition on chloride ingress. Chloride profiles in five different pastes are shown. Except from the silica fume addition, which is marked on the curves, the pastes are identical. The pastes have a water-cement ratio of 0.3 and have been chloride exposed for one month. The measurements are based on EPMA mapping. Anti leach samples.

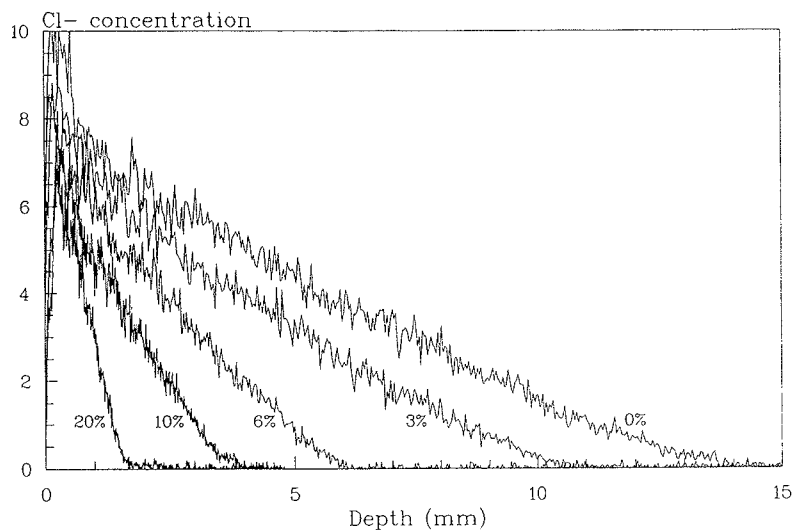


Figure 8. Influence of silica fume addition on chloride ingress. Chloride profiles in five different pastes are shown. Except from the silica fume addition, which is marked on the curves, the pastes are identical. The pastes have a water-cement ratio of 0.5 and have been chloride exposed for one month. The measurements are based on EPMA mapping.

3.9 INFLUENCE OF TEMPERATURE

Figure 9 and 10 show the influence of temperature on chloride ingress. An increased temperature is seen to accelerate the chloride ingress. This may mainly be caused by thermal activation of the diffusion process. However, chloride binding may partly contribute to the observed effect as well; The chloride binding is reduced when the temperature is increased³.

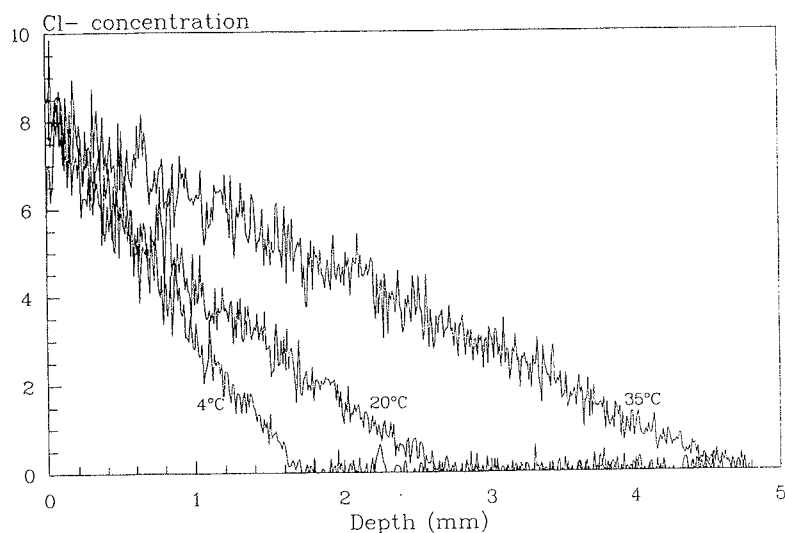


Figure 9. Influence of temperature on chloride ingress. Chloride profiles are shown for three identical cement pastes at $w/c=0.3$ without silica fume addition. The exposure temperature is marked on the curves. The pastes have been chloride exposed for one month. The measurements are based on EPMA mapping. Anti leach samples.

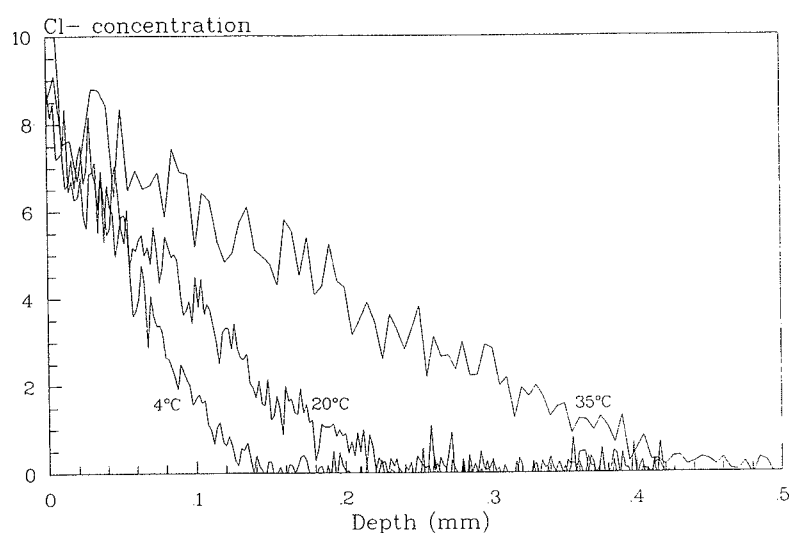


Figure 10. Influence of temperature on chloride ingress. Chloride profiles are shown for three identical cement pastes at $w/c=0.3$ with 20% silica fume addition. The exposure temperature is marked on the curves. The pastes have been chloride exposed for one month. The measurements are based on EPMA mapping. Anti leach samples. Note the resolution of the depth axis; the diameter of a typical cement particle is $10\text{ }\mu\text{m}$.

3.10 INFLUENCE OF EXPOSURE TIME

Figure 11 and 12 show the influence of exposure time on chloride ingress. Based on line scans, it was noted that the profiles for the exposure times considered, 1-180 days, have common intersection at the sample edge, depth 0 mm. This shows that:

1) The convective resistance for the chloride transport is negligible. The internal chloride transport in the cement paste is slow compared to the chloride transport through the surface boundary layer. That means, it is an internal transport phenomenon which is studied.

2) Chloride binding is fast relative to transport.

If the chloride binding were slow or the convective resistance had importance the profile intersection at the sample edge should increase with time.

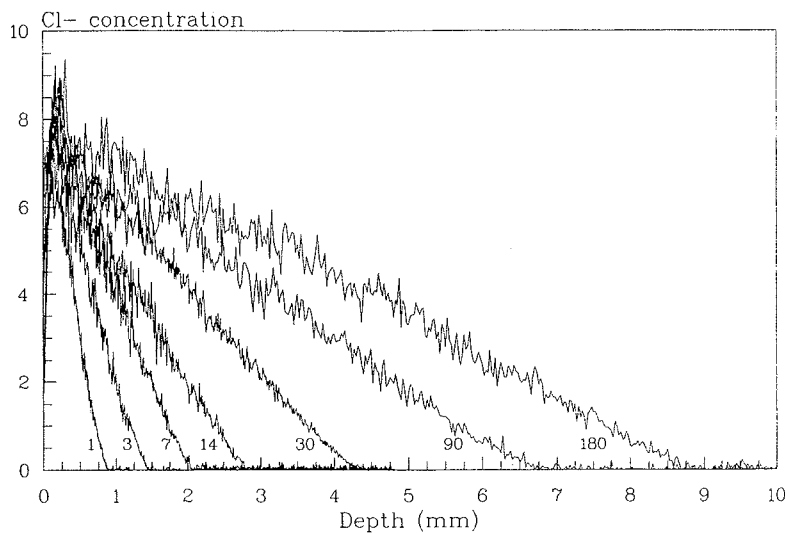


Figure 11. Influence of exposure time on chloride ingress. Chloride profiles are shown for seven identical cement pastes with $w/c=0.3$ without silica fume addition. The exposure time is marked on the curves. The measurements are based on EPMA mapping.

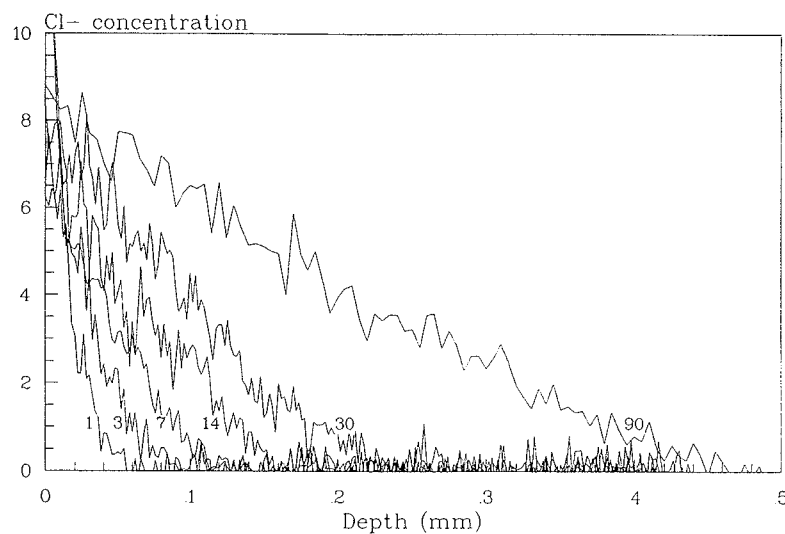


Figure 12. Influence of exposure time on chloride ingress. Chloride profiles are shown for six identical cement pastes with $w/c=0.3$ with 20% silica fume addition. The exposure time is marked on the curves. The measurements are based on EPMA mapping. Anti leach samples.

4 MODELLING

A literature review reveals that modelling of chloride ingress in cement paste is a very divisive subject^{28,29,33,35,37}. The cause for this seems to be that a major number of physical or chemical mechanisms may influence the chloride ingress.

The first mathematical model of chloride ingress into concrete^{18 p. 102} was published by Collepardi et al⁴³ in 1970. They used Fick's law for diffusion and calculated diffusion coefficients for various concrete compositions. Since then, Fick's law has been the basis for chloride ingress modelling, but a large number of modifications have been introduced. Unfortunately there is no general agreement on what modifications are the important ones. Some examples of these are:

□ The diffusion coefficient is concentration dependent²⁴. This observed concentration dependency may be the result of hydration of the chloride ions²⁷. The hydration may both enhance or hamper diffusion²⁷.

□ The chloride diffusion has to be balanced either by co-diffusion of oppositely charged ions, e.g. Na^+ or by counter-diffusion of identically charged ions, e.g. OH^- . This is referred to as multicomponent diffusion. This is one reason for the chloride diffusion to depend on the pore solution composition²⁸. Multicomponent diffusion can be described with a generalized form of Fick's law containing $(n-1)^2$ diffusion coefficients in a n -component system²⁷.

□ A significant amount of the ingressed chloride is immobilized through binding, either by adsorption on the C-S-H gel or by chemical reaction with the aluminate phases. More than 50% of the chloride in a cement paste may be bound. This delays the chloride ingress.

□ The chloride ingress may change the pore structure, and as a consequence as well modify the effective diffusion coefficient. It has both been suggested that the chloride ingress leads to a densification^{32,36} as well as a coarsening³⁹ of the pore structure.

The subject is further complicated by the fact that the transport process itself is debated. Physically adsorbed chloride may potentially move, but this surface diffusion is believed to be significantly slower than diffusion for the free chloride in the pore water³². In addition, the pore water of a cement paste cannot be considered bulk water; a part of the pore water is structured due to adsorption on the cement gel surface. This water may have a much higher viscosity⁴² than bulk water or act as an ionic screen³. For this reason only a part of the pore water may in reality serve as a transport medium for the chloride diffusion. Chatterji³⁸ suggests that the cations mainly diffuse along the pore surfaces whereas the anions diffuse through the bulk pore solution.

The mathematics of chloride ingress are very complicated. The basic Fick's law can be solved analytically, however, most modifications as those mentioned above prevent this. As an example, if Fick's law is combined with a chloride binding equation of the Freundlich type solutions for the modified diffusion equation can only be obtained by numerical methods^{31 p.122}.

At some level, the modelling will inevitably be a matter of neglect; Less important factors have to be neglected. The aim is to choose the smallest number of characteristics that, when combined, predict the most variation in behavior. A more complicated theory should not be introduced before it is very sure that it is needed.

4.1 COMPUTER PROGRAM FOR INGRESS MODELLING

The modelling which is performed in this project is based on single component Fick's diffusion modified with binding. The program which has been used to model the chloride ingress profiles is described and shown in Appendix E. The program is based on a first-order finite difference method.

In the program it is assumed that the transport of free chloride follows Fick's law for diffusion²⁷:

$$F = -D \frac{\partial c_f}{\partial x} \quad (4)$$

where F is the chloride ion flux [$\text{kg}/(\text{m}^2\text{s})$], c_f the free chloride concentration [kg/m^3] and x the ingress depth [m]. D is an effective diffusion coefficient [m^2/s] which takes into consideration the tortuosity of the pore system.

Ficks law of diffusion is a well-known and sound basis for describing chloride transport in cement paste systems. However, it is evident that the basic Fick's law alone is not able qualitatively to describe the chloride ingress. Experiments have shown that a large part of the chloride is bound in the cement paste. In the program, chloride binding is assumed to follow a Freundlich isotherm²¹ equation:

$$c_b = \alpha \cdot c_f^\beta \quad (5)$$

where c_b [$\text{mg}/\text{g-gel}$] is the bound chloride, c_f [$\text{mol Cl}/\text{l solution}$] is the free chloride and α and β are empirical constants. Note that the unit for c_f in the Freundlich equation is different from the unit for c_f in the diffusion equation. Unit conversion is, therefore, done throughout the program.

The chloride binding significantly modifies the shape of the chloride ingress profiles, as well as the calculated chloride diffusion coefficients, see Figure 13.

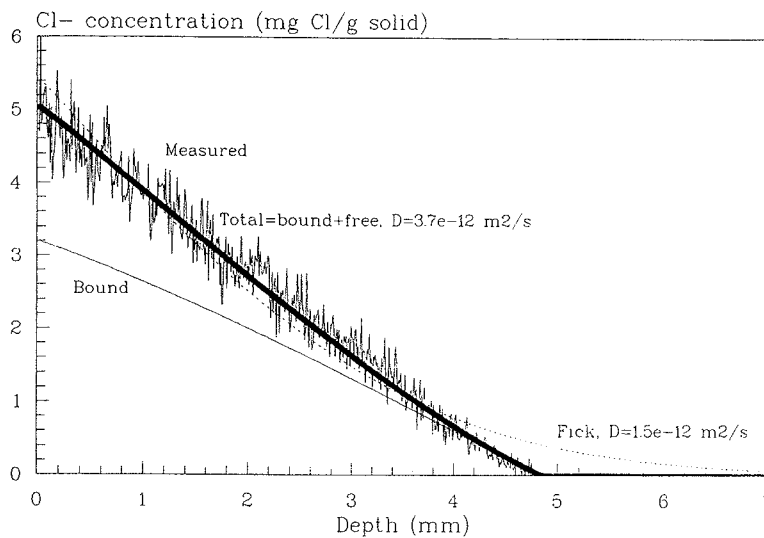


Figure 13. Example of measured and modelled chloride ingress profile. The paste has $w/c=0.3$, 0% sf. and has been chloride exposed for 30 days at 35°C . The fluctuating curve is the measured profile from EPMA mapping. The dashed line is calculated only from Fick's law with a diffusion coefficient of $1.5 \cdot 10^{-12} \text{ m}^2/\text{s}$. The wide line is calculated assuming that binding occurs. The amount of bound chloride for this profile is shown with the thin line. In this case, the diffusion coefficient for the free chloride is $3.7 \cdot 10^{-12} \text{ m}^2/\text{s}$.

As seen from Figure 13 the strongly concave shape of the Fick profile is qualitatively very different from the measurements; the measured profile is almost linear. If binding is included in the modelling the description of the measurements is substantially improved. In the case shown binding leads to an almost linear total profile. However, the curvature of the profile depends on the ratio of free to bound chloride. If the w/c ratio is increased relatively less chloride is bound, and the total profile will be more concave. A further account of this is given in Appendix D.

The full set of modelled and measured chloride profiles based on EPMA mapping are shown in

Appendix H. Only some of these will be shown further on. Input parameters for the calculations are shown in Appendix G.

The calculated profiles in Appendix H and Figure 13 have strong similarities with the measurements. At present, there seems to be no reason to include further mechanisms in the model. Despite this, two modifications were tested: 1) A chloride binding model which contained a combined Freundlich and Langmuir isotherm²¹, and 2) a delay on the establishment of chloride binding based on an exponential decay function with a half-time of 1 hour. These modifications did not lead to general improvements and have for this reason not been implemented in the present program. Actually, the fits were poorer when the chloride binding was assumed not to occur momentarily.

As discussed in the previous section there are several additional mechanisms which, in principle, could be taken into account for the chloride ingress model, for example, mobility of the bound chloride. However, this has not been done, because it is judged that these mechanisms are either too ill-described, or too complicated to implement in the modelling.

A general, quantitative verification of the modelled chloride ingress profiles has not been carried out in this project; The EPMA measurements are only semi-quantitative, c.f. section 2.14 and 3. For one sample a chloride profile was measured quantitatively by the traditional method ($w/c=0.5$, 0% silica fume, see Figure 4). The modelled profile shown in Appendix H estimates a chloride content about 25% lower than the measured amount by the traditional method. It has not been possible to clarify whether this is due to a systematic error on the traditional measurements or the modelled profile. More quantitative measurements should be carried out to examine this further.

4.2 CALCULATED DIFFUSION COEFFICIENTS

Table 4 shows modelled diffusion coefficients for the cement pastes. The modelled diffusion coefficients in Table 4 are seen to depend strongly on the composition of the cement paste. If the water-cement ratio is lowered or silica fume is added to the cement paste the diffusion coefficient diminishes. This will be discussed in more detail in section 4.3.

Anti leach samples are seen to have lower diffusion coefficients than the corresponding leached samples. For the sample at $w/c=0.3$ and 0% s.f. addition the diffusion coefficient is approximately 2.5 times lower when leaching is prevented. At 20% s.f. addition this diffusion coefficient ratio increases to about 6. However, if the leached zone, c.f. Appendix B, is considered completely open the diffusion coefficient ratio is approximately 2 independent of the silica fume addition. It is not known why the chloride ingress is faster when the samples are exposed to leaching. Possibly, counter diffusion of e.g. OH^- or a reduction of the chloride binding may account for this.

4.2.1 Influence of exposure time

From Table 4 it is seen that for a given cement paste the diffusion constant can be assumed independent of the exposure time. The systematic change with time, if any, is small in relation to the other parameters considered. Figure 14 and 15 shows experimental results and modelled chloride ingress profiles assuming that the diffusion coefficient is independent of the exposure time.

Paste		Chloride exposure time (days)							
w/c	% s.f.	1	3	7	14	30		90	180
0.2	0					0.80			
0.3	0	4.0	4.0	3.5	3.3	3.8	4°C: 0.85 20°C: 1.4 35°C: 3.7	3.5	3.1
	3					2.0	0.70		
	6					0.42	0.15		
	10					0.12	0.05		
	20	0.008	0.008	0.008	0.008	0.05	4°C: 0.004 20°C: 0.008 35°C: 0.028	0.012	
0.4	0					11			
0.5	0					22			
	3					13			
	6					4.2			
	10					1.6			
	20					0.30			
0.6	0					30			
0.7	0					36			

Table 4. Modelled diffusion coefficients, $D/(10^{-12} \text{ m}^2/\text{s})$, for the cement pastes. Bold-faced figures refer to anti leach samples. The exposure temperature is 20°C except for the four samples marked otherwise.

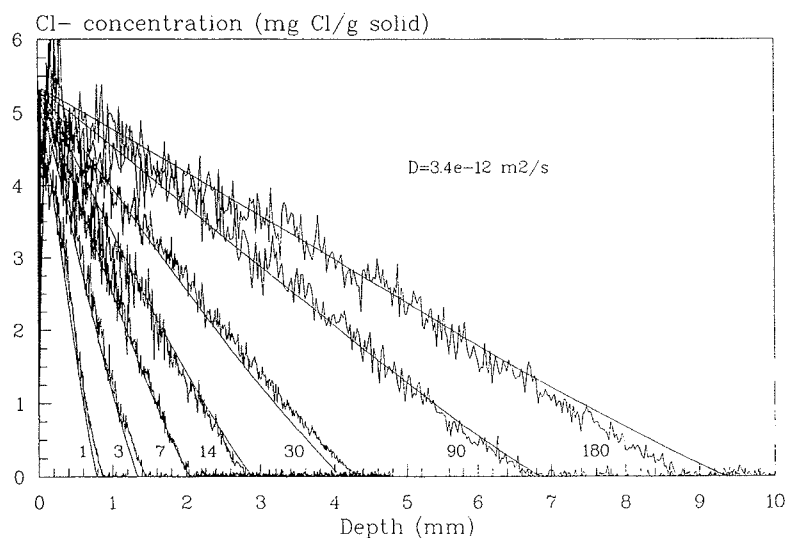


Figure 14. Influence of exposure time on chloride ingress. Chloride profiles are shown for seven identical cement pastes with $w/c=0.3$ without silica fume addition. The exposure time is marked on the curves. The fluctuating curves are measurements based on EPMA mapping. The smooth curves are calculated profiles with a diffusion coefficient of $D=3.4 \cdot 10^{-12} \text{ m}^2/\text{s}$.

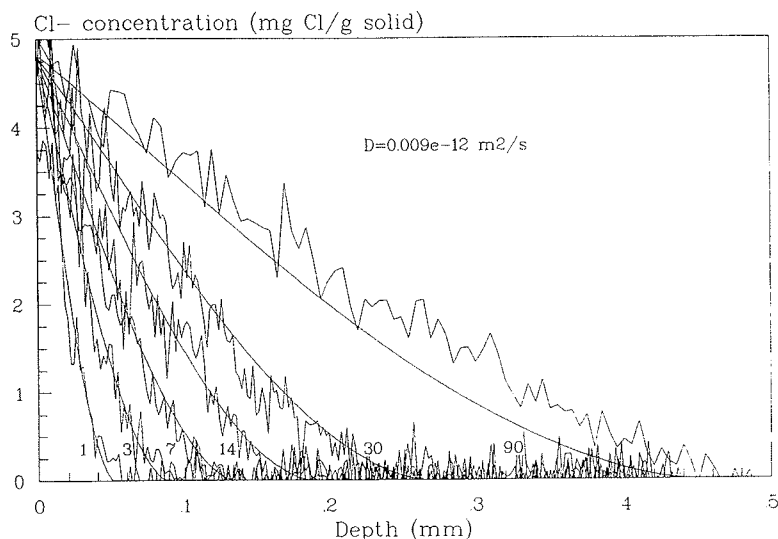


Figure 15. Influence of exposure time on chloride ingress. Chloride profiles are shown for six identical cement pastes with $w/c=0.3$ with 20% silica fume addition. The exposure time is marked on the curves. The fluctuating curves are measurements based on EPMA mapping. The smooth curves are calculated profiles with a diffusion coefficient of $D=0.009 \cdot 10^{-12} \text{ m}^2/\text{s}$.

4.2.2 Influence of temperature

Table 4 shows that the diffusion coefficient increases with the temperature. Figure 16 shows an Arrhenius plot from which the activation energy of chloride diffusion in two cement pastes can be evaluated.

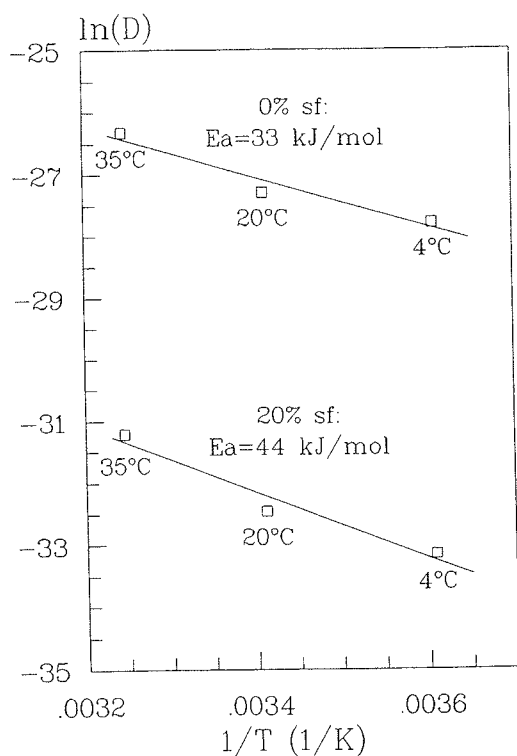


Figure 16. Arrhenius plot of modelled diffusion coefficients from Table 4. Activation energies of chloride diffusion for two cement pastes, both with $w/c=0.3$, but with different silica fume contents are calculated.

In Figure 16 the experimentally determined activation energies for chloride diffusion in the two cement pastes are calculated as 33 and 44 kJ/mol. This is in agreement with the range of values reported in the literature: Lambert et al⁴⁰ found an activation energy of 33 kJ/mol, Hansson et al¹⁴ gives values from 23 to 28 kJ/mol for well hardened pastes, Page and Lambert²⁶ 32 to 45 kJ/mol, Goto and Roy¹⁵ 50 kJ/mol and Collepardi et al¹³ 36 kJ/mol.

The activation energy for chloride diffusion in cement pastes, say 40 kJ/mol, is high compared to diffusion in bulk water. Chloride diffusion in pure water is known to be a thermally activated process with an activation energy of $E_a \approx 17$ kJ/mol, c.f. Appendix C. The reason for this difference is not known. However, it shows that chloride diffusion in cement paste is influenced by temperature dependent factors in addition to pure diffusion. Based on a comparison with oxygen diffusion it has been suggested that the phenomenon is caused by interaction between the chloride ion and the cement gel surface^{11,25,26,15}. So far, the temperature influence on the diffusion coefficient must be considered semi-empirical.

4.3 COMPOSITE THEORY

As noted in the previous section, the modelled diffusion coefficients depend strongly on the water-cement ratio and the silica fume addition. This is due to changes in the pore structure of the cement pastes. When the porosity is reduced or the tortuosity of the pore system is increased the diffusion coefficient will decrease.

Cement paste is a composite material; It is composed of several phases with different properties. In this project several simplified assumptions are made regarding the composite structure of the cement paste. These are given below.

From a diffusion point of view it may be convenient to consider a cement paste as composed by three phases, see Figure 17.

□ *Calcium hydroxide and unhydrated cement and silica fume.* These particles are considered impermeable to chloride ions, $D_{CH} = D_{ce} = D_{sf} = 0$ m²/s.

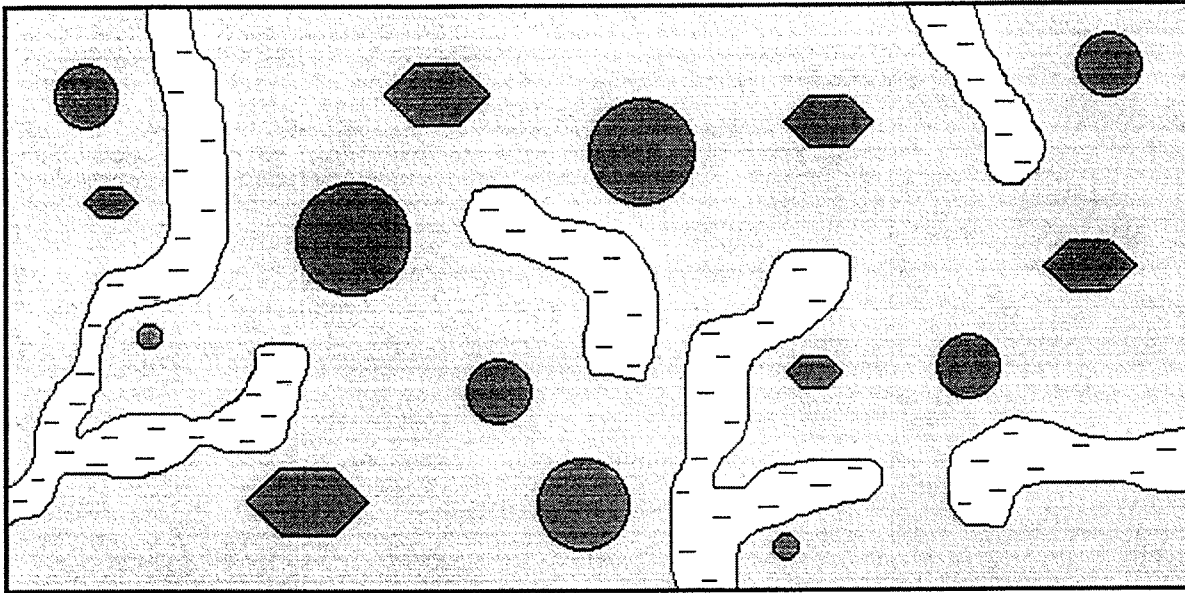
□ *Gel proper*, i.e. gel solid and gel water. It is assumed that a bulk diffusivity can be assigned to the gel proper. Garboczi⁹ has suggested the diffusion coefficient of the gel proper to be 1/400 of the diffusion coefficient in bulk water, i.e. $D_{gp} \approx 5 \cdot 10^{-12}$ m²/s at 20°C. However, it may depend on the cement type or silica fume addition³⁴.

□ *Capillary water.* It is assumed that the chloride diffusion coefficient in the capillary water is identical to that of bulk water, $D_{cw} = 1.81 \cdot 10^{-9}$ m²/s at 20°C.

The composite model is further simplified by assuming that the calcium hydroxide and the unhydrated cement and silica fume exist as discrete inclusions in the continuous gel proper phase. These two phases make up the *gel matrix*. The diffusion coefficient of the gel matrix, D_{gm} , is calculated from the Maxwell equation (2), c.f. section 3.6:

$$D_{gm} = D_{gp} \frac{2 \left(1 - \frac{V_{ce} + V_{sf} + V_{CH}}{V_{ce} + V_{sf} + V_{CH} + V_{gp}} \right)}{2 + \frac{V_{ce} + V_{sf} + V_{CH}}{V_{ce} + V_{sf} + V_{CH} + V_{gp}}} = D_{gp} \frac{V_{gp}}{V_{gp} + \frac{3}{2} (V_{ce} + V_{sf} + V_{CH})} \quad (6)$$

Where V_{ce} , V_{sf} , V_{CH} and V_{gp} is the volume of unhydrated cement, unhydrated silica fume, calcium hydroxide and gel proper respectively.







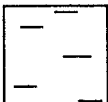
PHASES			Relative diffusivity
1	 Gel matrix	A   Calcium hydroxide, unhydr. cement + sf	0
		B  Gel proper: Gel solid, gel water	1/400 ?
2	 Water-filled capillaries		1

Figure 17. Simplified illustration of a cross section in a cement paste. The cement paste is considered a composite material consisting of the following phases: 1) The gel matrix and 2) the water-filled capillaries. The gel matrix itself is subdivided into: A) Calcium hydroxide, unhydrated cement and unhydrated silica fume and B) gel proper. Calcium hydroxide, unhydrated cement and unhydrated silica fume are assumed to be impermeable to chloride. The effective chloride diffusion coefficient of gel proper is suggested by Garboczi⁹ to be 400 times lower than for chloride diffusion in the capillary pores.

Despite the above simplifications it is not straightforward to calculate the diffusion coefficient of the cement paste. Numerous different composite theoretical models which attempt to predict a physical property of a two phase composite material can be found in the literature¹⁰. These models are derived from a known phase geometry. The above mentioned Maxwell equation is one example of such a model which assumes one phase to be discrete, periodically spaced spheres.

The geometry of the capillary pore system of a cement paste is very complex. No attempt has been made in this project to evaluate the capillary pore geometry, and establish a composite theoretical model based on this. The approach used here has been to compare the measuring results with different composite theoretical models. From this examination it was concluded that the following model, which is derived for phase symmetric crumbled foil composites¹⁰, gives the best description:

$$D_p = D_{gm} \cdot \frac{n + 2\sqrt{n} \cdot [1 + c \cdot (n-1)]}{n + 2\sqrt{n} - c \cdot (n-1)} \quad (7)$$

where D_p is the effective diffusion coefficient of the paste, $n = \frac{D_{cw}}{D_{gm}}$ and c is the capillary porosity,

$$c = \frac{V_{cw}}{V_{cw} + V_{gm}} = \frac{V_{cw}}{V_{cw} + V_{gp} + V_{ce} + V_{sf} + V_{CH}}$$

The input data for equation (7) as well as calculated diffusion coefficients are given in Table 5. The modelled data apply to leached samples.

w/c	0.2	0.3	0.4	0.5	0.6	0.7
$V_{ce} + V_{CH}$	0.471	0.347	0.276	0.234	0.208	0.188
V_{gp}	0.522	0.610	0.607	0.566	0.504	0.455
V_{cw}	0.007	0.043	0.117	0.201	0.287	0.357
D_{CH}, D_{ce}, D_{sf}	0					
D_{gp}	$1.00 \cdot 10^{-12}$					
D_{cw}	$1.81 \cdot 10^{-9}$					
D_{gm}	$4.25 \cdot 10^{-13}$	$5.39 \cdot 10^{-13}$	$5.94 \cdot 10^{-13}$	$6.17 \cdot 10^{-13}$	$6.17 \cdot 10^{-13}$	$6.17 \cdot 10^{-13}$
D_p	$0.8 \cdot 10^{-12}$	$3.3 \cdot 10^{-12}$	$9.0 \cdot 10^{-12}$	$17 \cdot 10^{-12}$	$27 \cdot 10^{-12}$	$36 \cdot 10^{-12}$
D_p measured	$0.8 \cdot 10^{-12}$	$3.8 \cdot 10^{-12}$	$11 \cdot 10^{-12}$	$22 \cdot 10^{-12}$	$30 \cdot 10^{-12}$	$36 \cdot 10^{-12}$

Table 5. Calculated diffusion coefficients for different cement pastes without silica fume addition ($V_s=0$) based on volumes and assumed diffusion coefficients for single phases. The volume of the phases have been calculated with Powers' simplified model⁴ assuming the degrees of hydration given in Appendix G. The measured diffusion coefficients for the pastes are from Table 4.

According to the composite modelling in Table 5 the diffusivity of the gel matrix only varies slightly as a function of the water-cement ratio. That means, the diffusivity of plain cement paste is mainly determined by the capillary porosity, whereas the degree of hydration seems to be a less important parameter. This is in agreement with Garboczi and Bentz³⁴. The diffusion coefficient for the gel proper used in Table 5 is about five times lower than the value suggested by Garboczi⁹. The reason for this discrepancy is not known.

When silica fume is added to the cement pastes significantly lower diffusion coefficients are measured, c.f. Table 4. With the applied composite theoretical model this can only be achieved if the bulk diffusivity of the gel proper is reduced by the silica fume addition. Garboczi and Bentz³⁴ have previously speculated whether this may be the case. This may be due to modifications of the pore structure or ion interaction with the C-S-H formed by the pozzolanic reaction of silica fume with calcium hydroxide.

Figure 18 shows diffusion coefficients plotted as a function of the capillary porosity.

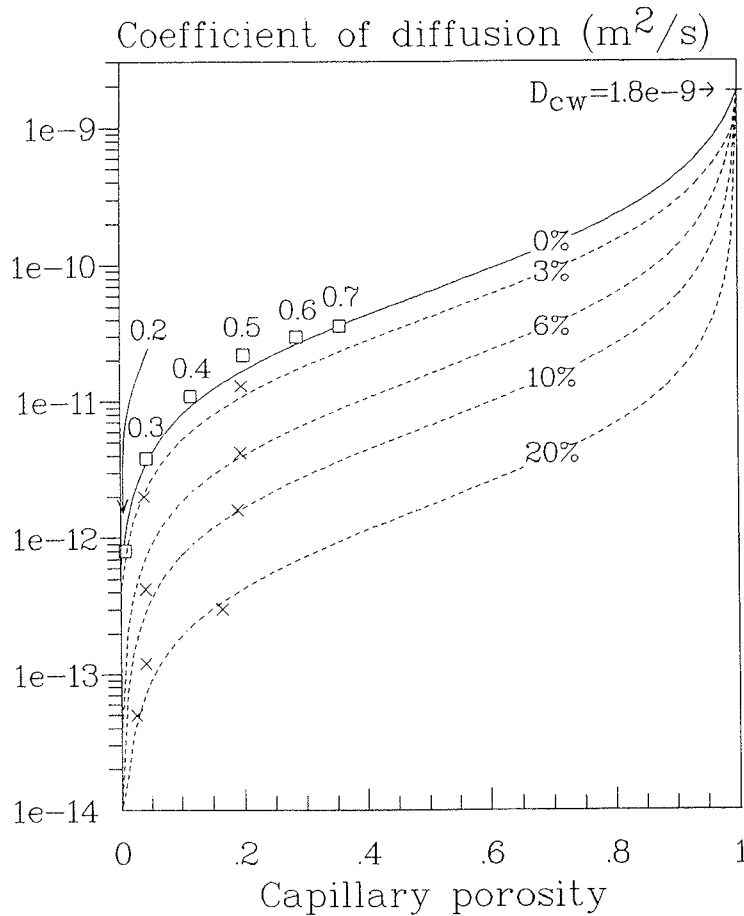


Figure 18. Diffusion coefficients as a function of the capillary porosity. Boxes and crosses are measured values from Table 4. As marked, the boxes represent different w/c ratios at 0% silica fume addition. The crosses represent different silica fume additions at w/c ratios 0.3 and 0.5. The solid line is calculated with equation (7) for a gel matrix diffusivity of $6.2 \cdot 10^{-13} \text{ m}^2/\text{s}$, and a capillary water diffusivity of $1.8 \cdot 10^{-9} \text{ m}^2/\text{s}$, given as intersections at capillary porosities 0 and 1 respectively. The dashed lines suggest courses for different silica fume additions corresponding to gel matrix diffusivities of $4 \cdot 10^{-13}$, $3.5 \cdot 10^{-14}$, $6 \cdot 10^{-15}$ and $4 \cdot 10^{-16} \text{ m}^2/\text{s}$.

It requires further studies to examine whether the composite model parameters have a physical meaning. According to the composite model the diffusion coefficient of the gel proper depends very strongly on the silica fume addition; By addition of 20% silica fume it is reduced by a factor of 1000. However, this may be a pure mathematical representation. The reduction in the diffusion coefficient caused by silica fume addition may, partly, be due to a reduced connectivity of the capillary pore system.

The geometric interpretation of the composite model, if any, is that the shape of the capillary pore system can be described as shell like inclusions in the surrounding gel matrix.

5 CONCLUSION

This report deals with chloride ingress in cement paste and mortar measured with Electron Probe Micro Analysis, EPMA. Approximately 50 different cement paste and mortar samples are examined ranging from traditional to modern high-performance types. The pastes and mortars are exposed to synthetic seawater from 1 day to half a year.

The measuring results have been modelled with a computer program which simulates chloride ingress in cement paste. The program assumes that chloride is transported by mono-component diffusion according to Fick's law, that chloride is bound by the cement gel according to a Freundlich isotherm and that Powers' simplified model describes the phase distribution of a cement paste. The simulated ingress profiles closely resemble the measurements. At the present there seems to be no reason to include further mechanisms in the model.

The experiments show that both the composition of the paste or mortar as well as the exposure conditions have a strong influence on the chloride ingress. The parameters examined included:

Exposure conditions: Leaching, temperature and exposure time.

Paste or mortar composition: Superplasticizer, mixing technique, aggregate, water-cement ratio and silica fume addition.

Of the more important observations it can be noted that quartz aggregate addition to cement paste can be considered a pure dilution effect from a chloride ingress point of view. Comparison of mortar and cement paste profiles, furthermore, indicate that internal micro cracking due to autogenous shrinkage has no overall effect on the chloride ingress.

From the measurements with varying exposure times it seems that the diffusion coefficient can be considered a constant for a given cement paste; It does not depend on exposure time nor on the ingress depth. The influence of the temperature on the diffusion coefficient for two cement pastes has been described with activation energies of 33 and 44 kJ/mol. For the tightest cement pastes leaching of the cement gel may have a very significant influence on the chloride ingress.

The influence of water-cement ratio and silica fume addition has been simulated with a composite theoretical model. According to the composite model the measured change in diffusion coefficient as a function of the water-cement ratio can be related solely to the capillary porosity of the pastes. Contrary to this, the observed strong reduction of the diffusion coefficient when silica fume is added may be due to a change of the gel proper or a reduced connectivity of the capillary pore system.

5.1 FURTHER RESEARCH

In continuation of or supplementary to the present project a number of further examinations would be interesting. Some of these are mentioned below:

- ☐ Attempts should be made to make the EPMA measuring technique quantitative.
- ☐ It should be examined why leaching results in a higher diffusion coefficient, c.f. section 4.2.
- ☐ A more thorough composite theoretical investigation of diffusivity of cement pastes should be carried out. Does the suggested composite model have a geometric/physical meaning - can other material properties, such as e.g. strength, be modelled with the same equation?
- ☐ To what extent is bound chloride mobile? Will this have implications for the calculated ingress profiles? May this explain the odd energy of activation for chloride diffusion, c.f. section 4.2.2. Can this, in addition, be the reason for the necessary modification of the β -parameter in the Freundlich equation, c.f. Appendix G?
- ☐ The assumption that a certain part of the pore fluid is inaccessible for chloride ions needs further clarification, c.f. Appendix E and G.

Appendix A

PREPARATION OF CHLORIDE EXTRACTION LIQUID

This appendix describes the preparation of a chloride extraction liquid. The chloride extraction liquid can be used for measurement of the chloride content in cement paste with a chloride selective electrode, for example as in Germann's RCT test (Rapid Chloride test).

The following recipe has been used²⁰:

350 ml distilled water
50 ml concentrated (minimum 65%) nitric acid, HNO_3
104.5 g sodium acetate trihydrate, $\text{CH}_3\text{COONa} \cdot 3\text{H}_2\text{O}$

A number of comparative experiments have shown that the extraction liquid gives the same results as Germann's RCT extraction liquid²⁰.

The sodium acetate also exists in a water-free state. However, this is not stable and should, therefore, not be used. The extraction liquid is acidic in order to dissolve the chloride. According to professor Ernst Maahn (Department of Manufacturing Engineering, Technical University of Denmark) this also reduces measurement errors from influencing ions other than chloride. The brochure for the chloride selective electrode (Radiometer) states that the measurements are influenced particularly from sulfide, S^{2-} . Germann's extraction liquid contains a strong sulfid precipitator for this reason. According to professor Ernst Maahn this is unnecessary because concrete is unlikely to contain sulfide.

Appendix B

LEACHING DURING CHLORIDE EXPOSURE

According to Taylor²² a cement paste is not stable in pure water. Pure water will remove alkali hydroxides, dissolve CH and decompose the hydrated silicate and aluminate phases. The ultimate residue will consist essentially of hydrous forms of silica, alumina and iron oxide, all the CaO having been lost. This is a consequence of a 1000 times lower solubility for SiO₂ than for CaO.

The chloride binding capacity of a cement paste is proportional to the amount of cement gel²¹. Disappearance of the cement gel due to leaching, therefore, leads to a reduced chloride binding capacity.

In the present study leaching was not anticipated to have a major influence on the chloride profiles. Consequently no attempts were, initially, made to avoid this, except from keeping the amount of exposure liquid low. However, on a number of profiles leaching has a very significant effect. Figure B1 shows an example.

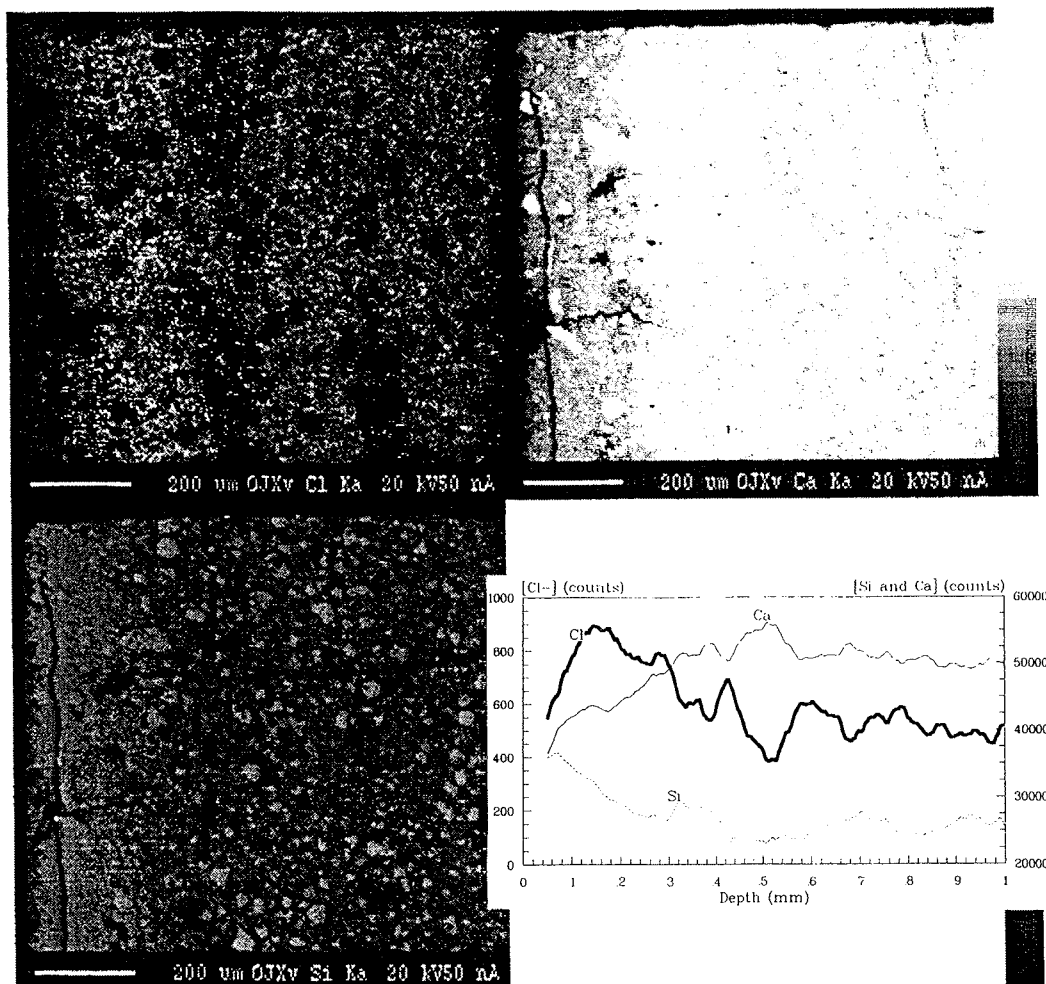


Figure B1. EPMA measurements of Cl, Si and Ca demonstrating the effect of leaching. Three element maps and a graph based on line scans are shown. The left surface is the chloride exposed surface. The cement paste has a w/c=0.3, 0% silica fume and has been chloride exposed for 14 days. Due to the low water-cement ratio the cement paste contains a large amount of unhydrated cement particles. These are identified as spots high in Si and Ca and low in Cl. The degree of hydration is approximately 0.7 according to measured amounts of chemically bound water.

By EPMA only the relative amounts of elements are measured. This is believed to be the reason for the observed increase in Si in the leached zone of Figure B1; When Ca is removed by leaching the total mass is lowered. Since CaO may compose e.g. 2/3 of the cement paste by mass this has a quite significant effect. A calculation shows that the measured increase in Si can be fully accounted for by the drop in Ca. Therefore, the volumetric Si concentration is not believed to increase in the leached zone.

The leaching of the cement gel results in a reduced chloride binding capacity. This results in a distortion of the chloride profile close to the exposed surface. A selection of the samples were examined by EPMA mapping. Based on this, it was possible to estimate the thickness of the leached zone, see Table B1.

Paste			Chloride exposure time (days)						
w/c	% s.f.	SPC	1	3	7	14	30	90	180
0.2	0	+					0.12		
0.3	0	+	0.11	0.17	0.20	0.26	0.32	0.40	0.40
	3	+					0.24		
	6	+					0.20		
	10	+					0.18		
0.4	0	÷					0.50		
0.5	0	÷					0.65		
	3	÷					0.45		
	6	÷					0.25		
	10	÷					0.24		
	20	÷					0.23		
0.6	0	÷					0.80		
0.7	0	÷					0.95		

Table B1. Thickness of leached zone (mm) for cement pastes estimated from Si EPMA mapping. Exposure temperature: 20°C.

As seen from Table B1 the thickness of the leached zone increases systematically with the w/c-ratio and the exposure time.

To avoid leaching some special exposure liquids were prepared: a large amount of crushed cement paste was submerged for several months in the NaCl exposure liquid before onset of the chloride ingress experiment. Apart from the NaCl the exposure liquid will thus be in equilibrium with the pore fluid of the cement paste which is subsequently exposed. No leaching could be observed in these cement pastes.

INFLUENCE OF DRYING ON CHLORIDE REMOVAL

The Cl map in Figure B1 shows that the drying technique does not lead to chloride removal. Both the top and the left surface are drying surfaces; the top surface is cut immediately after the chloride exposure is concluded. If the chloride was removed due to the drying (wick action) there should be a change in the chloride concentration towards the top surface. However, no such effect can be seen.

Three different drying techniques have been tested: silica gel drying, vacuum drying and freeze drying.

EPMA line scans and mapping was performed parallel to the direction of drying to check whether the drying leads to a measurable chloride removal. The sample in Figure B1 has been vacuum dried.

The time of drying should be short compared to the chloride exposure time. If not, the chloride will diffuse during the drying process and, thus, change the chloride profile after the chloride exposure has been concluded. For the samples exposed for 1 day the drying should take at maximum 1-2 hours. In this connection drying means removal of water to a level where the chloride is fixed. As an alternative freeze drying can be used. During freeze drying the chloride cannot move. If freeze drying is used the time to freeze the water in the samples should be less than 1-2 hours.

At short chloride exposure times only freeze and vacuum drying are potentially useful. At long chloride exposure times, e.g. more than 14 days, silica gel drying can also be used.

The samples for freeze drying are freeze dried to -40°C immediately after cutting. After at least 1 day at -40°C the samples are freeze dried at approximately -50°C and $p < 1$ mbar. At -40°C all the capillary water will be frozen. The amount of unfrozen water in the gel pores will be very small and will have a very high viscosity. Therefore, no significant chloride removal can take place. An estimate shows that ordinary deep freezer temperature, -18°C , is sufficiently low to fix the chloride ions in a cement paste.

Vacuum drying at $p < 1$ mbar is performed at room temperature with a rotary pump for 1 day immediately after cutting. After vacuum and freeze drying the samples are stored with fresh silica gel for 1 week followed by one further day of evacuation.

Based on measurements of the weight loss during drying the following drying times have been found sufficient:

Freeze drying: 5 days freeze drying removes approximately 100% of the evaporable water; 2 days is insufficient. The time for freezing the water in the samples is not known - a couple of hours before the chloride is fixed is probably realistic.

Silica gel drying: Fixation of the chloride ions takes at least 1 day, presumably a couple of days. 1 day drying removes approximately 4-30% of the evaporable water for the samples examined - the densest pastes are slowest dried. Complete drying takes weeks.

Vacuum drying: After 2 hours vacuum drying more than 10% of the evaporable water is removed from the densest paste: $w/c=0.3$, 20% silica fume. 1 day of vacuum drying removes more than 50% of the evaporable water.

According to EPMA line scans and maps none of the three drying techniques leads to chloride removal. Vacuum drying was checked most thoroughly since this technique was the most suitable; vacuum drying is fast and simple and can be used as well for short chloride exposure times.

Appendix C

DIFFUSION AND VISCOSITY

Diffusion and viscosity are from a physical point of view related. This can be illustrated by, for example, a chloride ion which diffuses through water. The water molecules have to move when the chloride ion moves. If the viscosity of the water is high the coefficient of diffusion must be low. Furthermore, if the diffusing ion is large the coefficient of diffusion must be low, because the ion will have a large hydraulic drag. This is expressed in the *Stokes-Einstein relation*:

$$D = \frac{k \cdot T}{6\pi \cdot \eta \cdot r} \quad (C1)$$

Where D is the coefficient of diffusion [m^2/s], k is the Boltzmanns constant ($1.381 \cdot 10^{-23} \text{ J/K}$), T is the Kelvin temperature [K], η is the viscosity [$\text{kg}/(\text{m} \cdot \text{s})$] and r is the hydrodynamic radius of the molecule [m].

The Stokes-Einstein relation is valid, if the diffusing molecule is large relative to the molecules in the media of diffusion. If the size of the molecules are comparable the numeric constant in expression (C1) will change⁵ from 6 to approximately 4.

As an example the coefficient of diffusion for the chloride ion in water can be calculated at 25°C :

$$D_{\text{Cl}^- \text{ in } \text{H}_2\text{O}} = \frac{1.318 \cdot 10^{-23} \cdot 298.15}{4\pi \cdot 0.89 \cdot 10^{-3} \cdot 1.81 \cdot 10^{-10}} = 1.94 \cdot 10^{-9} \frac{\text{m}^2}{\text{s}}$$

Where the ionic radius of the chloride ion, $1.81 \cdot 10^{-10} \text{ m}$, is used as the hydraulic radius. A table lookup gives^{6 p. 832} $D_{\text{Cl}^- \text{ in } \text{H}_2\text{O}} = 2.03 \cdot 10^{-9} \frac{\text{m}^2}{\text{s}}$.

Theoretically supported experiments show that the temperature dependence of the viscosity of water can be described by^{6 p. 595}

$$\eta = \eta_0 \cdot \exp\left(\frac{E_{a,\eta}}{R \cdot T}\right) \quad (C2)$$

Where $E_{a,\eta}$ is the energy of activation of viscosity [J/mol].

An analogous thermal dependence will be valid for the diffusion process⁵.

$$D = D_0 \cdot \exp\left(\frac{-E_{a,D}}{R \cdot T}\right) \quad (C3)$$

Where $E_{a,D}$ is the energy of activation of the diffusion coefficient [J/mol].

The following calculation shows how the activation energy of viscosity is related to the activation energy of the diffusion coefficient. Insertion of (C1) in (C3) gives:

$$\frac{k \cdot T}{6\pi \cdot \eta \cdot r} = \frac{k \cdot T_0}{6\pi \cdot \eta_0 \cdot r} \cdot \exp\left(\frac{-E_{a,D}}{R \cdot T}\right)$$

Using (C2) in this expression and reduction gives:

$$E_{a, D} = E_{a, \eta} - R \cdot T \cdot \ln \left(\frac{T}{T_0} \right) \quad (C5)$$

In the temperature range 0-50°C the correction term $R \cdot T \cdot \ln \left(\frac{T}{T_0} \right)$ will numerically be lower than approximately 200 J/mol. In this temperature range the activation energy for chloride diffusion in water⁷ is approximately 17 kJ/mol, or approximately 100 times larger than the correction term. Fitting of viscosity data around room temperature with (C2) gives an activation energy for the viscosity of water⁸ of approximately 17 kJ/mol.

For diffusion of ions in aqueous solution a good approximation is:

$$E_{a, D} \approx E_{a, \eta} \quad (C6)$$

Appendix D

INFLUENCE OF WATER-CEMENT RATIO ON SIGNIFICANCE OF CHLORIDE BINDING

Traditionally, chloride ingress in concrete has been modelled as a pure transport phenomenon, i.e. chloride binding in the cement paste has been neglected. This may be an acceptable approximation for traditional concretes with high water-cement ratios. However, for modern concretes with low water-cement ratios the chloride binding has a significant effect on the chloride ingress. This is demonstrated in the following.

Based on Powers' simplified model⁴ the following phase composition of two cement pastes can be calculated, see Table D1.

w/c	α (%)	Gel solid including CH (kg/m ³)	Capillary water (m ³ /m ³)	Gel water (m ³ /m ³)	Accessible water (m ³ /m ³)
0.7	0.87	1072	0.357	0.162	0.454
0.2	0.52	1254	0.000	0.189	0.113

Table D1. Examples of phase composition for two different cement pastes. The degrees of hydration, α , have been measured by loss on ignition. The amounts of phases have been calculated with Powers' simplified model⁴, assuming the cement pastes to be fully water saturated. See text for further explanation.

Experiments have indicated that a part of the gel water is inaccessible for dissolution of chloride. At room temperature this part seems to correspond to approximately one monolayer of water on the gel surface, which constitutes 40% of the gel water. Based on this, the total amount of accessible water has been calculated in Table D1.

Suppose that the two cement pastes are in equilibrium with a 3% NaCl solution, and that the chloride binding can be described with a Freundlich isotherm,

$$c_b = \alpha c_f^\beta$$

Where c_b [mg/g-gel] is the bound chloride, c_f [mol Cl/l solution] is the free chloride and α and β are empirical constants, $\alpha=6.9$ and $\beta=0.40$.

Since

$$3\% \text{ NaCl} \sim \frac{30 \text{ g/l}}{58.44 \text{ g/mol}} = 0.51 \frac{\text{mol}}{\text{l}} \sim 0.51 \frac{\text{mol}}{\text{l}} \cdot 35.45 \frac{\text{g}}{\text{mol}} = 18.20 \frac{\text{g Cl}}{\text{l}}$$

the amounts of bound chloride respectively free chloride in the two cement pastes can be calculated, see Table D2:

w/c	Free chloride (kg Cl/m ³ paste)	Bound chloride (kg Cl/m ³ paste)	Total chloride (kg Cl/m ³ paste)
0.7	8.3 (59%)	5.7 (41%)	13.9
0.2	2.1 (24%)	6.6 (76%)	8.7

Table D2. Amounts of bound and free chloride in the two cement pastes from Table D1 when brought in equilibrium with 3% NaCl. The amounts relative to the total chloride are given in brackets.

As can be seen from Table D2 the different phase compositions of two cement pastes have a strong influence on the relative amounts of free and bound chloride. At a high water-cement ratio the chloride mainly exist as free chloride whereas bound chloride is the major phase at a low water-cement ratio.

In traditional concretes at high water-cement ratios it may be an acceptable approximation to neglect binding. However, at low water-cement ratios chloride binding has to be taken into account, since it significantly alters the chloride ingress. In such cases a chloride ingress model purely based on Ficks law of diffusion is inadequate.

Appendix E

The following pages show a Turbo Pascal 7.0 program "DIFBIND.PAS". The program has been used for calculation of chloride ingress profiles in cement pastes. Basically, the program contains three elements:

1. Calculation of the cement paste phase composition according to Powers' simplified model. A description of the model can be found in the literature⁴.
2. Transport of free chloride according to Fick's law:

$$F = -D \frac{\partial c_f}{\partial x}$$

where F is the chloride ion flux [kg/(m²s)], c_f the free chloride concentration [kg/m³] and x the ingress depth [m]. D is an effective diffusion coefficient [m²/s] which takes into consideration the tortuosity of the pore system. Due to mass conservation it can be seen that:

$$\frac{\partial c_f}{\partial t} = - \frac{\partial F}{\partial x}$$

The first-order finite difference approximation to this equation is:

$$\begin{aligned} c_f(x, t_{i+1}) &= c_f(x, t_i) + \Delta c_f(x, t_i) \\ &= c_f(x, t_i) + D \frac{\Delta t}{(\Delta x)^2} \cdot [c_f(x - \Delta x, t_i) + c_f(x + \Delta x, t_i) - 2 \cdot c_f(x, t_i)] \end{aligned}$$

3. Chloride binding according to the Freundlich isotherm²¹ equation:

$$c_b = \alpha \cdot c_f^\beta$$

where c_b [mg/g-gel] is the bound chloride, c_f [mol Cl/l solution] is the free chloride and α and β are empirical constants. Note that the unit for c_f in the Freundlich equation is different from the unit for c_f in the diffusion equation. Unit conversion is, therefore, done throughout the program, c.f. PROCEDURE "freundlich" in the program. The chloride binding equilibrium is established for every element after each finite difference calculation step.

It is assumed that a certain fraction of the gel water is inaccessible for dissolved chloride ions. This fraction is set to 40% of the gel water at 20°C, 55% at 4°C and 28% at 35°C, c.f. Appendix G. This corresponds to the amount of water held by the cement paste when brought to equilibrium at 11% relative humidity. At 20°C this equals approximately 1 mono layer of water on the surface of the gel solid¹².

The program considers semi-infinite and one-dimensional chloride ingress. However, for memory and calculation time reasons the number of elements is finite. If chloride reaches the deepest element it is assumed to accumulate in the cement paste.

The program is based on a first-order finite difference method. This type of numerical solution is susceptible to calculation instability and inaccuracy. The program does not examine whether this may be the case for a given set of input data, but parameters which can be used to avoid these difficulties are suggested.

```

(*-----*)
(*  CALCULATION OF CHLORIDE INGRESS PROFILES IN CEMENT PASTE  *)
(*  *)
(*  -The transport of free chloride ions is assumed to follow  *)
(*  Ficks law  *)
(*  -Chloride binding is assumed to follow a Freundlich isotherm *)
(*  -The phase composition is assumed to follow Powers simplified *)
(*  model  *)
(*  -A certain fraction of the gel water is assumed to be  *)
(*  inaccessible for dissolved chloride ions.  *)
(*  1 mono layer of water on the surface of the gel solid  *)
(*  represent approximately 40% of the gel water.  *)
(*  *)
(*  One-dimensional chloride ingress is considered  *)
(*  *)
(*  Ole Mejlhede Jensen, March 1998  *)
(*-----*)

PROGRAM difbind;

{$N+} (* 8087 mode activated in order to enable double precision *)

(*-----*)
(*  Definition of global quantities  *)
(*-----*)

uses
    crt;

const
    cnil = 18.20; (* exposure concentration in kg/m3 water = 3% NaCl *)
    max = 500; (* maximum number of elements in conc. vectors *)
    u = 0.40; (* 40% of the gel water is inaccessible for
               dissolved chloride ions *)
    (* t05 = 60; half-life for chloride binding is put to
               60 minutes, which equals binding of 7% during
               6 minutes *)

type
    vector = array(.1..max.) of double;

var
    (* counters *)
    i,j,t: integer;
    (* Parameters for Powers model *)
    wc, sc, alfa_c, alfa_s: double;
    vol_uhyd_c, vol_uhyd_s, vol_gel_water, vol_cap_water: real;
    vol_csh_gel, vol_ch_gel: double;
    mas_uhyd_c, mas_uhyd_s, mas_gel_water, mas_cap_water: real;
    mas_csh_gel, mas_ch_gel: double;
    (* Parameters for Ficks transport *)
    d, ttot, dt, xt看, dx: double;
    nt, nx: integer; (* number of time and dimensional elements *)
    (* Parameters for Freundlich isotherm *)
    alpha, beta: double;
    alphaf: double;
    (* If establishment of the chloride binding equilibrium is
       assumed to follow an exponential decay function, the following
       parameter should be included:
       dec: real; Decremental factor: in every time step the amount
       of bound will increase due to diffusion of free
       chloride. The Decremental factor indicate how far
       the new equilibrium is attained. At a decremental
       factor of 0 no binding occurs; dec=1 represent a
       momentaneous chloride binding; dec=0.05 indicate
       that the amount of bound chloride has changed 5%
       from the old amount to the new amount *)
    f, b: double; (* factors for unit conversion *)
    (* concentration vectors: vectors with suffix _f have
       the unit [kg Cl/m3 accessible pore fluid] others
       [kg Cl/kg solid] *)
    ctot, cbound, cfree, ocfree, cfree_f, ocfree_f: vector;

```

```

(*-----*)
(*  data entry                                     *)
(*-----*)
PROCEDURE entry;

begin
  (* Parameters for Powers model *)
  Writeln('PASTE COMPOSITION:');
  Writeln('input water-cement ratio: ');
  Readln(wc);
  Writeln('input silica-cement ratio: ');
  Readln(sc);
  Writeln('input the degree of cement hydration (0<alfa<1): ');
  Readln(alfa_c);
  Writeln('input the degree of silica fume hydration (0<alfa<1)');
  Readln(alfa_s);

  (* Parameters for Ficks transport *)
  Writeln('DIFFUSION:');
  Writeln('input the effective coefficient of diffusion: ');
  Writeln(' (Unit: m2/s)');
  Readln(d);
  Writeln('input maximum depth of ingress (accumulation in last element: ) ');
  Writeln(' (Unit: mm)');
  Readln(xtot);
  Writeln('input element size (at maximum ',max,' elements)');
  Writeln(' (Unit: mm)');
  Readln(dx);
  xt看ot:=xtot/1000;
  dx:=dx/1000;
  Writeln('input exposure time: ');
  Writeln(' (Unit: days)');
  Readln(ttot);
  ttot:=ttot*60*60*24;
  Writeln('To avoid instability or slow calculation speed the Fourier step');
  (* If the Fourier step is higher than app. 0.5 instability occurs *)
  Writeln('should be approximately 0.25. This corresponds to a time step of');
  Writeln('0.25/d*dx*dx/60/60:7:4, ' hours');
  Writeln('input the time step per calculation cycle: ');
  Writeln(' (Unit: hours)');
  Readln(dt);
  dt:=dt*60*60;

  (* Parameters for Freundlich isotherm *)
  Writeln('CHLORIDE BINDING:');
  Writeln('input the Freundlich parameter alfa: ');
  Writeln(' (Unit for free chloride: mol/l, bound: mg/g-gel)');
  Readln(alfahf);
  Writeln('input the Freundlich parameter beta: ');
  Readln(beta);
  Writeln('Calculation in progress - please wait....');
end;

(*-----*)
(*  INITIALIZATION OF VARIOUS PARAMETRS          *)
(*-----*)
PROCEDURE initialization;

begin
  (*
  dec:=1-exp(ln(0.5)/(t05*60)*dt); *)
  nx:=round(xtot/dx);  (* number of elements in the conc. vector *)
  nt:=round(ttot/dt);  (* number of time steps *)
  (* reset various conc. vectors *)
  for i:=1 to nx do
  begin
    ctot[i]:=0;
    cbound[i]:=0;
    cfree[i]:=0;
    ocfree[i]:=0;
    cfree_f[i]:=0;
    ocfree_f[i]:=0;
  end;
end;
end;

```



```

(*-----*)
(*  CALCULATION OF PHASE COMPOSITION ACCORDING TO POWERS MODEL  *)
(*-----*)
PROCEDURE powers;

var  chem_water_c: real;
     chem_sh: real;
     ini_mas_c, ini_mas_s: real; (* initial masses of ce and sf *)
     theta: real; (* Initial porosity, auxillary figure *)

const rho_c=3100;
      rho_s=2200;
      rho_w=1000;
      rho_ch=2240;
      chem_sh_c=6.5e-5;
      chem_sh_s=22e-5;
      c_c=0.26;      (*chemical bound water, cem. hydration, g/g*)
      c_s=0;         (*do for silica fume*)
      v_gel_c=0.19;  (*amount of gel water in cem. hydr. prod.*)
      v_gel_s=0.5;   (*do for silica fume*)
      ch_c=0.387;    (*CH production from cement hydr., g/g*)
      ch_s=1.48;     (*CH consumption of silica fume: 1.2 mol CH per mol S*)

BEGIN
  theta:=wc/(wc+rho_w/rho_c+rho_w/rho_s*sc);
  ini_mas_c:=theta/wc*rho_w;
  ini_mas_s:=sc*ini_mas_c;
  vol_uhyd_c:=theta/wc*rho_w/rho_c*(1-alfa_c);
  mas_uhyd_c:=vol_uhyd_c*rho_c;
  vol_uhyd_s:=(1-theta-theta/wc*rho_w/rho_c)*(1-alfa_s);
  mas_uhyd_s:=vol_uhyd_s*rho_s;
  mas_gel_water:=(ini_mas_c-mas_uhyd_c)*v_gel_c
    +(ini_mas_s-mas_uhyd_s)*v_gel_s;
  vol_gel_water:=mas_gel_water/rho_w;
  chem_sh:=(ini_mas_c-mas_uhyd_c)*chem_sh_c+(ini_mas_s-mas_uhyd_s)*chem_sh_s;
  chem_water_c:=(ini_mas_c-mas_uhyd_c)*c_c;
  mas_cap_water:=theta*rho_w-chem_water_c-mas_gel_water+chem_sh*rho_w;
  (*note: open system!*)
  vol_cap_water:=mas_cap_water/rho_w;
  mas_ch_gel:=(ini_mas_c-mas_uhyd_c)*ch_c-(ini_mas_s-mas_uhyd_s)*ch_s;
  vol_ch_gel:=mas_ch_gel/rho_ch;
  mas_csh_gel:=(ini_mas_c-mas_uhyd_c)*(1+c_c)
    +(ini_mas_s-mas_uhyd_s)-mas_ch_gel;
  vol_csh_gel:=1-vol_uhyd_c-vol_uhyd_s-vol_gel_water
    -vol_cap_water-vol_ch_gel;
END;

(*-----*)
(*  CALCULATION OF PARAMETERS FOR FREUNDLICH ISOTHERM  *)
(*-----*)
PROCEDURE freundlich;

BEGIN
  (* Conversion factor for free chloride: from [kg Cl/kg solid]
    to [kg Cl/m3 accessible pore fluid] *)
  f:=(mas_uhyd_c+mas_uhyd_s+mas_ch_gel+mas_csh_gel)
    /(vol_cap_water+(1-u)*vol_gel_water);
  (* Conversion factor for bound chloride: from [kg Cl/kg solid]
    to [kg Cl/kg CSH solid] *)
  b:=(mas_uhyd_c+mas_uhyd_s+mas_ch_gel+mas_csh_gel)
    /(mas_csh_gel+mas_ch_gel);
  (* calculation of alfa-parameter for other units in
    Freundlich expression (the beta-parameter in unchanged)*)
  alpha:=alfahf/1000/b*exp(beta*ln(f/35.45));
end;

(*-----*)
(*  DIFFUSION OF FREE CHLORIDE  *)
(*-----*)
PROCEDURE diffusion;

BEGIN
  (* Old conc-vector is storred *)

```

```

for i:=1 to nx do
begin
  ocfree_f[i]:=cfree_f[i];
  ocfree[i]:=cfree[i];
end;
(* First element is handled separately *)
cfree_f[1]:=ocfree_f[1]
+dt/dx/dx*d*(0.5*cnil+ocfree_f[2]-3/2*ocfree_f[1]);
For i:=2 to (nx-1) do
begin
  cfree_f[i]:=ocfree_f[i]+dt/dx/dx*d
    *(ocfree_f[i-1]+ocfree_f[i+1]-2*ocfree_f[i]);
end;
(* Last element: accumulation! *)
cfree_f[nx]:=ocfree_f[nx]
+dt/dx/dx*d*(ocfree_f[nx-1]-ocfree_f[nx]);
For i:=1 to nx do
Begin
  (* free chloride in [kg Cl/kg solid] is calculated *)
  cfree[i]:=cfree_f[i]/f;
end;
END;

(*-----*)
(* BINDING OF CHLORIDE *)
(*-----*)
PROCEDURE binding;

var
  ctoti, cfreei: double; (* iteration concentrations *)
  alfacfreeibeta: double; (* calculation variable *)

BEGIN
  For i:=1 to nx do
  Begin
    (* The total amount of chloride in an element is
       calculated *)
    ctoti[i]:=cfree[i]+cbound[i];
    (* Now, the totale amount of chloride is distributed
       between free and bound. Since this cannot be done
       analytically, an iterative procedure is used.
       The iteration is controlled by the sum of free and
       bound chloride which must equal the total amount.
       In order to save calculation time the parameter ctoti
       is introduced: *)
    ctoti:=ctoti[i];
    (* A starting estimate for the free chloride concentration
       is the old chloride concentration: *)
    cfreei:=cfree[i];
    (* It is no use to waste time on elements with a very low
       free chloride concentration (possible 0), and in addition
       it causes problems with the logarithm function: *)
    if cfreei>1e-20 then
    begin
      for j:=1 to 10 do (* 10 New-Rap reskursions *)
      begin
        alfacfreeibeta:=alpha*exp(beta*ln(cfreei));
        cfreei:=cfreei*(1-(alfacfreeibeta+cfreei-ctoti)
          /(alfacfreeibeta+cfreei));
      end;
    end;
    cfree[i]:= (* cfree[i]-dec*(cfree[i] - *) cfreei (* ) *) ;
    cbound[i]:=ctoti[i]-cfree[i];
    cfree_f[i]:=cfree[i]*f;
  end;
end;

(*-----*)
(* SCREEN PRINT OF PROFILES *)
(*-----*)
PROCEDURE screen_print;

var

```

```

time, x, tot, free, bound: real;

Begin
time:=t/nt*ttot/60/60/24 (* time in days is calculated *);
writeln('-----');
writeln('time: ',time:5:2,' days');
writeln('x (mm) [Cl]:tot free bound (mg/g solid) ');
writeln('-----');
for i:=1 to nx do
begin
x:=(xtot*i/nx-1/2*xtot/nx)*1000;
tot:=ctot[i]*1000;
free:=cfree[i]*1000;
bound:=cbound[i]*1000;
writeln(x:6:3,' ',tot:8:5,' ',free:8:5,' ',bound:8:5);
end;
end;

(*-----*)
(* FILE PRINT OF PROFILES *)
(*-----*)
PROCEDURE file_print;

var
outputfil: text;
filename: string[80];
time, x, tot, free, bound: real;

Begin
writeln('input file name for saving data (full directory adress): ');
readln(filename);
assign(outputfil,filename);
rewrite(outputfil);
time:=t/nt*ttot/60/60/24;
writeln(outputfil,'w/c=',wc,' s/c= ',sc);
writeln(outputfil,'Degree of hydr. for cement:',alfa_c,' and silica fume
',alfa_s);
writeln(outputfil,'Effective coefficient of diffusion: ',d,' m2/s');
ttot:=ttot/60/60/24;
writeln(outputfil,'Exposure time: ',ttot,' days');
dt:=dt/60/60;
writeln(outputfil,'time steps per calculation cycle: ',dt,' hours');
xtot:=xtot*1000;
writeln(outputfil,'Maximum ingress depth: ',xtot,' mm');
dx:=dx*1000;
writeln(outputfil,'Element size: ',dx,' mm');
writeln(outputfil,'Freundlich parameter alfa: ',alphaf,' and beta: ',beta);
writeln(outputfil,'x (mm) [Cl]:tot free bound (mg/g solid) ');
for i:=1 to nx do
begin
x:=(xtot*i/nx-1/2*xtot/nx);
tot:=ctot[i]*1000;
free:=cfree[i]*1000;
bound:=cbound[i]*1000;
writeln(outputfil,x:6:3,' ',tot:8:5,' ',free:8:5,' ',bound:8:5);
end;
close(outputfil);
end;

(*-----*)
(* MAIN PROGRAM *)
(*-----*)
Begin
entry;
initialization;
powers; (* calculation of phase composition *)
freundlich; (* calculation of chloride binding *)
for t:=1 to nt do
begin
diffusion;
binding;
end;
screen_print;
file_print;
end.

```

Appendix F

This section shows measuring results of exposure liquid pH and degree of hydration for the leached samples after chloride exposure, see Table F1. The degree of hydration of the cement is measured from weight loss at 105-1050°C. The degree of hydration is calculated based on the assumption that silica fume does not bind water chemically and that the amount of chemical bound water per gram of hydrated cement is 0.25 gram.

The degree of hydration of the silica fume was measured³ to approximately 80% by ²⁹Si MAS NMR on a sample with w/c=0.5 and 10% silica fume addition.

Paste			Chloride exposure time (days)						
w/c	% s.f.	SPC	1	3	7	14	30	90	180
0.2	0	+					0.53 11.9		
0.3	0	+	0.69 11.3	0.72 11.5	0.69 11.7	0.70 -	0.73 12.1	0.75 12.4	0.78 12.0
	3	+					0.71 12.0		
	6	+					0.67 11.9		
	10	+					0.67 11.7		
	20	+	0.61 10.7	0.65 11.1	0.63 11.3	0.66 -	0.65 11.6	- 11.9	0.70 11.5
0.4	0	÷					0.83 12.3		
0.5	0	+					- 12.3		
	3	+					0.84 12.2		
	6	+					0.78 12.1		
0.5	0	÷					0.90 12.3		
	3	÷					0.85 12.2		
	6	÷					0.82 12.0		
	10	÷					0.82 11.9		
	20	÷					0.80 11.7		
0.6	0	÷					0.89 12.3		
0.7	0	÷					0.88 12.4		

Table F1. Degrees of hydration of the cement in the chloride exposed samples (left) and pH of exposure liquid (right, bold figures).

Due to the chloride exposure these samples will contain NaCl, which may partly evaporate during ignition (melting point: 801°C, boiling point: 1413°C). Therefore, the degrees of hydration in Table F1 may, potentially, be slightly higher than the true values. Based on an approximate calculation the calculated degree of hydration will at maximum be 5% too high (for complete chloride ingress in a cement paste at w/c=0.7). However, as shown by the following argument the measurements in Table F1 indicate that the degree of hydration is not influenced by chloride.

For the samples at w/c=0.3 an increase in the degree of hydration can be observed with the exposure time. Furthermore, this increase seems to be independent of the silica fume addition; approximately 9% during 180 days of exposure. From the EPMA measurements it is known that the silica fume addition causes a substantial difference in the amount of chloride ingress. This indicate that the degree of hydration is not influenced by chloride. The increase in degree of hydration is believed to be due to further hydration of the cement.

Appendix G

This section shows input parameters for the chloride ingress modelling. These include degrees of hydration, Table G1, and chloride binding constants, Table G2. The number of depth elements chosen was 100 for all runs. The number of time elements was approximately 1000 to 20.000 depending on the paste composition.

Paste		Chloride exposure time (days)						
w/c	% s.f.	1	3	7	14	30	90	180
0.2	0					0.51		
0.3	0	0.68	0.69	0.69	0.69	0.71	0.73	0.75
	3					0.70		
	6					0.68		
	10					0.66		
	20	0.61	0.61	0.61	0.62	0.64	0.66	0.67
0.4	0					0.82		
0.5	0					0.87		
	3					0.85		
	6					0.83		
	10					0.81		
	20					0.79		
0.6	0					0.87		
0.7	0					0.87		

Table G1. Degrees of hydration of the cement and silica fume used in the chloride ingress modelling. The values have been estimated based on the measurements reported in Appendix F. In Table F1 an increase in the measured degree of hydration is observed as a function of the exposure time. The values in the above table take this into account.

Temp. (°C)		wt-% silica fume addition				
		0	3	6	10	20
4°C	α	8.0	8.0	8.0	8.0	8.0
	β	0.50	0.51	0.53	0.55	0.60
	u_i	54%	54%	54%	54%	54%
20°C	α	7.0	7.0	7.0	7.0	7.0
	β	0.50	0.51	0.53	0.55	0.60
	u_i	40%	40%	40%	40%	40%
35°C	α	6.0	6.0	6.0	6.0	6.0
	β	0.50	0.51	0.53	0.55	0.60
	u_i	28%	28%	28%	28%	28%

Table G2. Freundlich isotherm parameters used in the chloride ingress modelling. α and β refer to the Freundlich isotherm form: $c_b = \alpha \cdot c_f^\beta$, where the units for c_b and c_f are [mg/g-gel] and [mol Cl/l solution] respectively. u_i [%] is the fraction of the gel water which is inaccessible for the dissolved chloride ions³.

The values in Table G2 are based on measurements reported in another project³. However, in the modelling it was observed that if a higher β -parameter was used than the one found in the chloride binding experiments³, the modelled chloride ingress profiles fitted the measurements much better. At 0% silica fume addition $\beta=0.4$ was found from linear regression, whereas $\beta=0.5$ has been used in the modelling, c.f. Table G2.

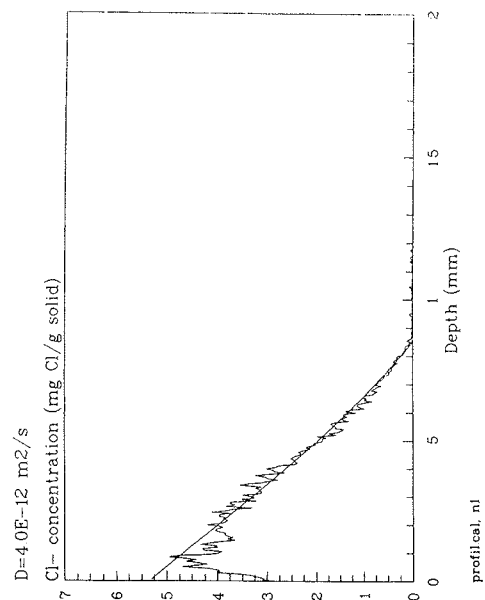
It is not known why the modelling is improved by increasing the β -parameter. One reason may be that the measured β only applies to chloride concentrations in the range app. 0.01-0.5 mol/l, whereas β increases at lower concentrations¹². Since the modelling concerns the full concentration range 0-0.5 mol/l an increased β may take this into account. Another explanation may be that the reduced chloride binding which is implied by the reduced β -parameter simulates mobility of the bound chloride.

In any case, the mentioned modification of the β -parameter did not change the estimated diffusion coefficient.

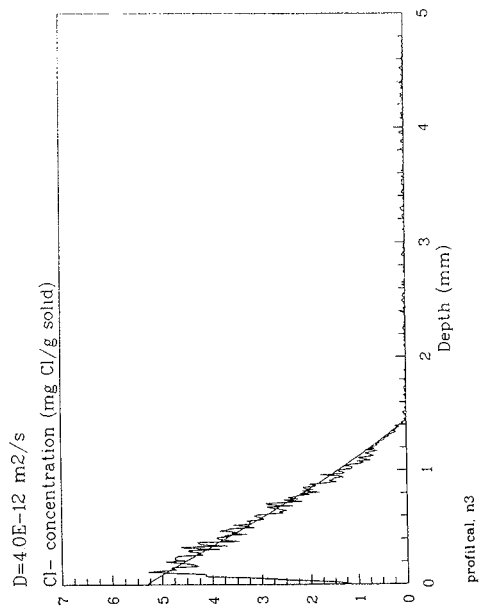
Appendix H

This section shows modelled and measured chloride profiles based on EPMA mapping. The computer program shown in Appendix E and the input parameters shown in Appendix G have been used to produce the modelled curves.

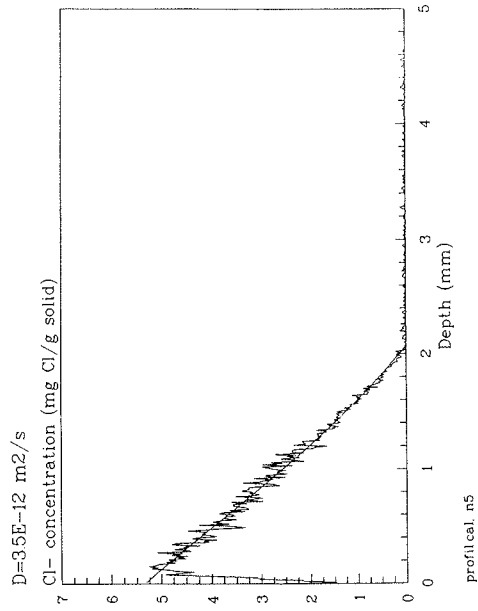
w/c=0.3, 0% sf, 1 day, 20°C



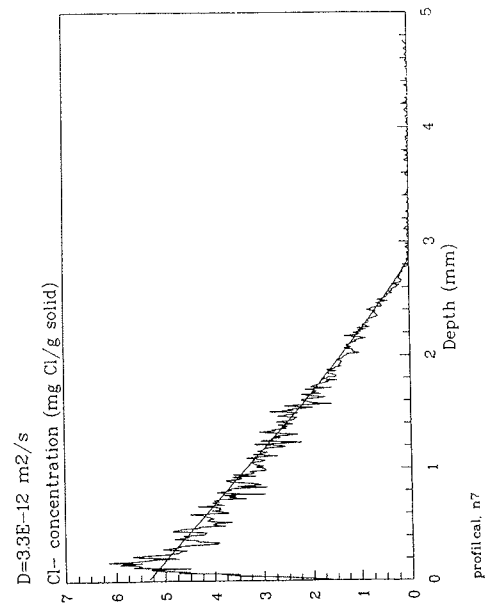
w/c=0.3, 0% sf, 3 days, 20°C



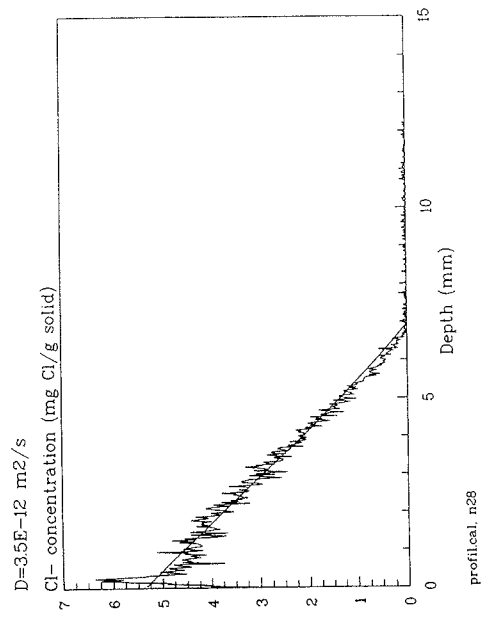
w/c=0.3, 0% sf, 7 days, 20°C



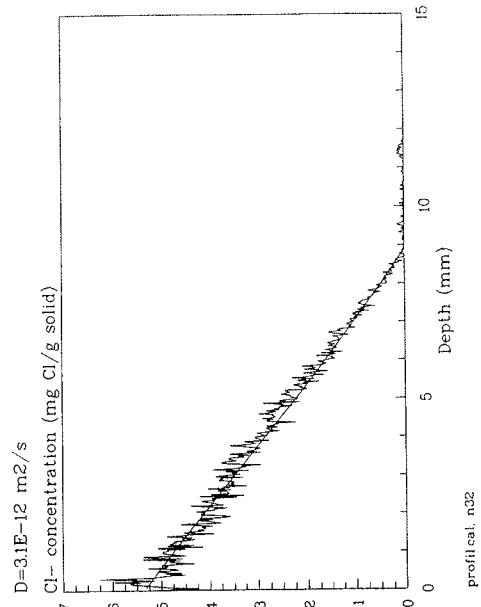
w/c=0.3, 0% sf, 14 days, 20°C



w/c=0.3, 0% sf, 90 days, 20°C

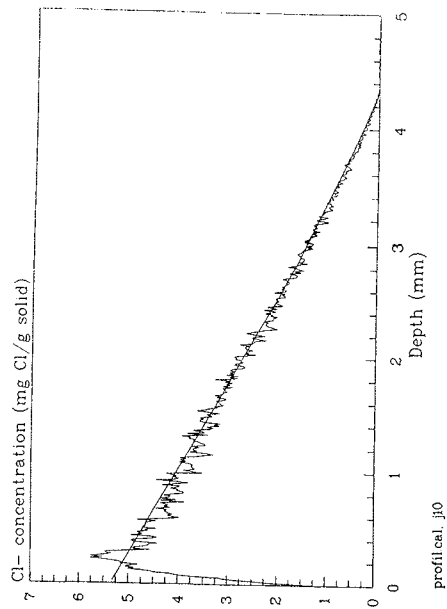


w/c=0.3, 0% sf, 180 days, 20°C



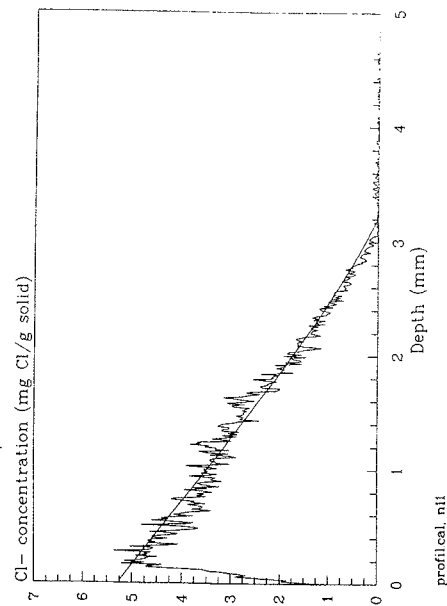
w/c=0.3, 0% sf, 30 days, 20°C

D=38E-12 m²/s



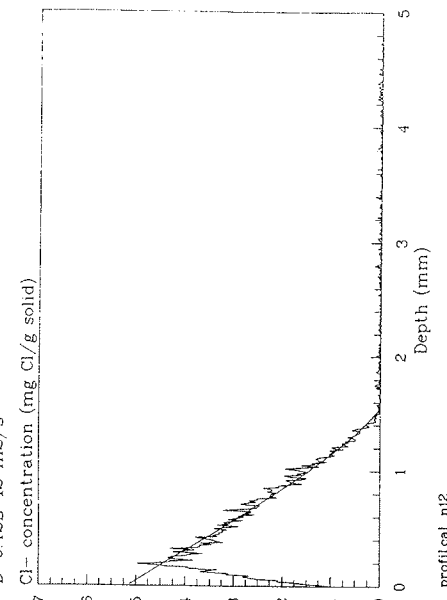
w/c=0.3, 3% sf, 30 days, 20°C

D=20E-12 m²/s



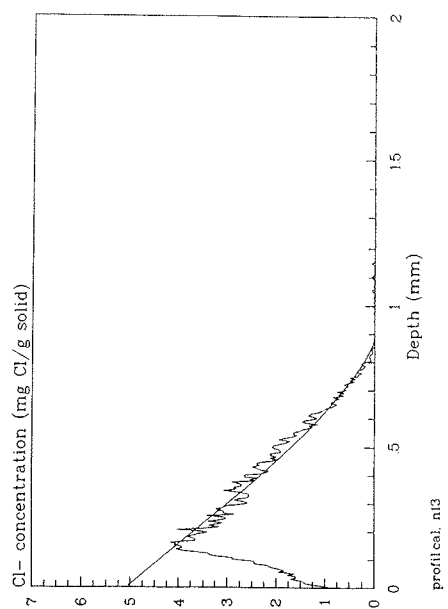
w/c=0.3, 6% sf, 30 days, 20°C

D=0.42E-12 m²/s



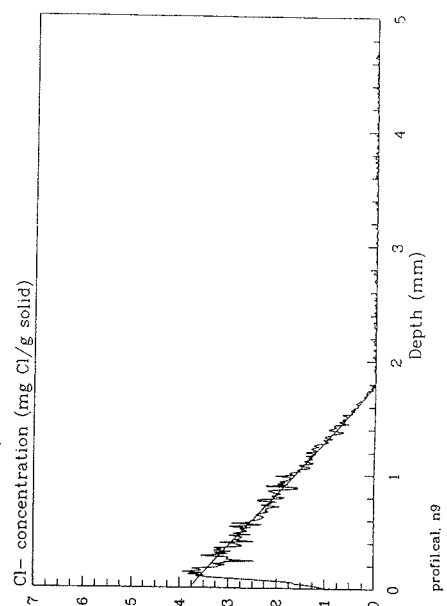
w/c=0.3, 10% sf, 30 days, 20°C

D=0.12E-12 m²/s



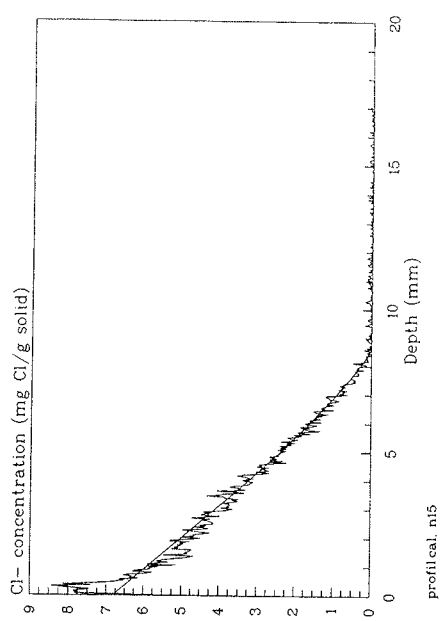
w/c=0.2, 0% sf, 30 days, 20°C

D=0.80E-12 m²/s

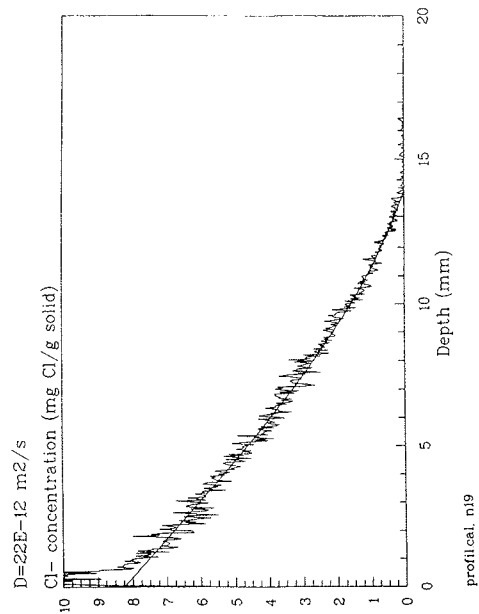


w/c=0.4, 0% sf, 30 days, 20°C

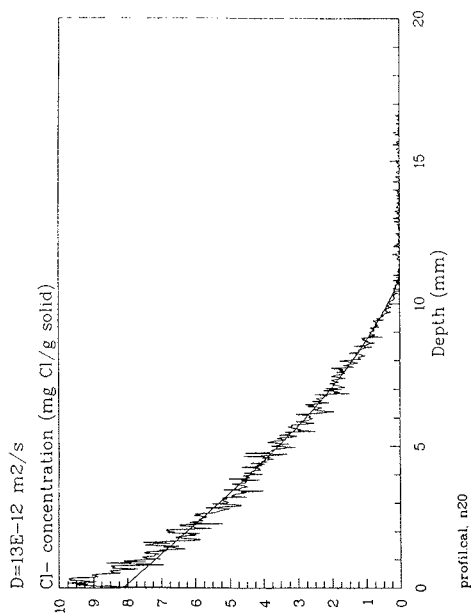
D=11E-12 m²/s



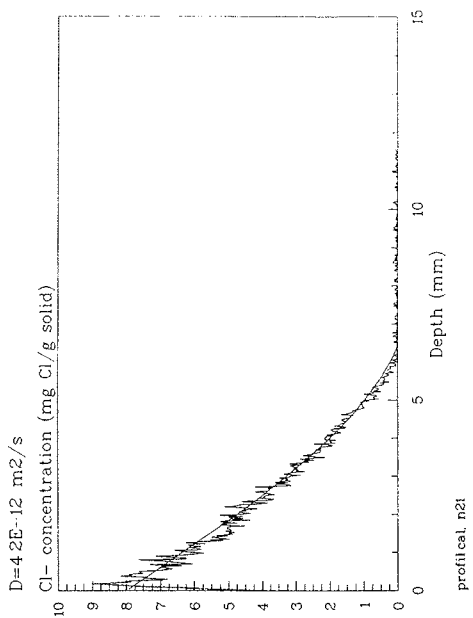
w/c=0.5, 0% sf, 30 days, 20°C



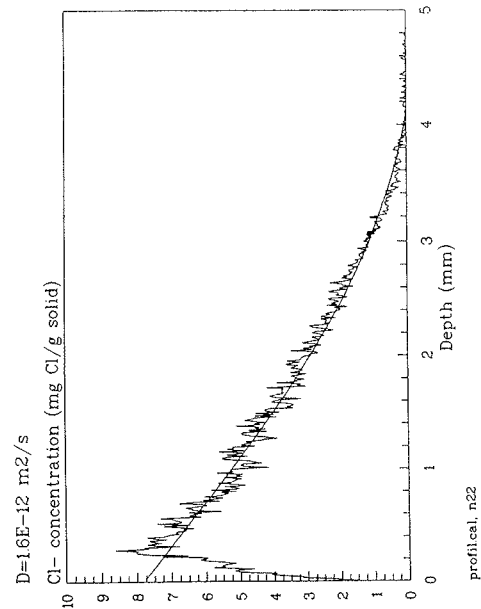
w/c=0.5, 3% sf, 30 days, 20°C



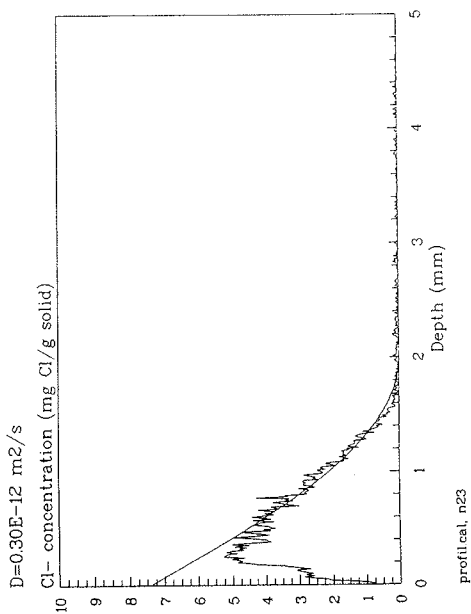
w/c=0.5, 6% sf, 30 days, 20°C



w/c=0.5, 10% sf, 30 days, 20°C

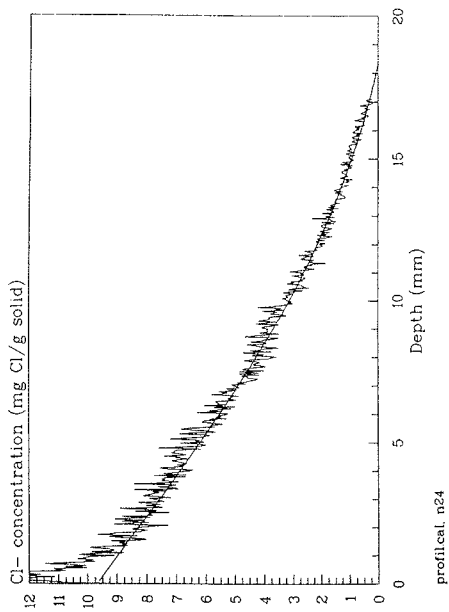


w/c=0.5, 20% sf, 30 days, 20°C



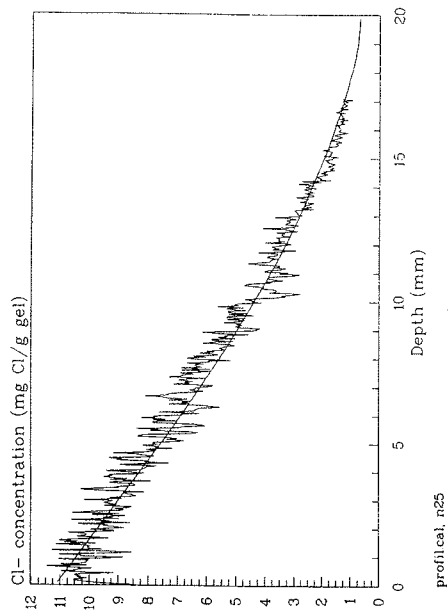
w/c=0.6, 0% sf, 30 days, 20°C

D=30E-12 m²/s



w/c=0.7, 0% sf, 30 days, 20°C

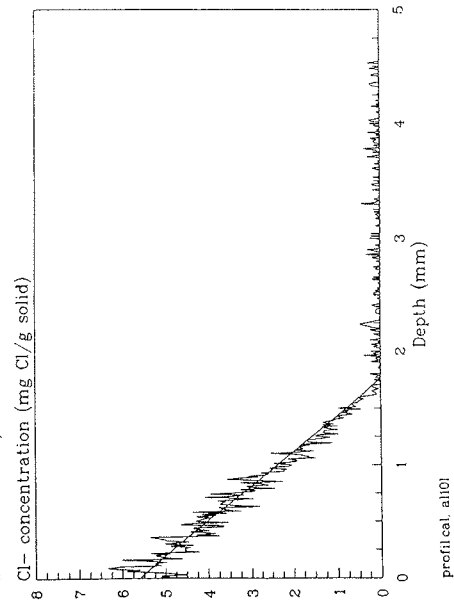
D=36E-12 m²/s



w/c=0.3, 0% sf, 30 days, 4°C

Anti-leach

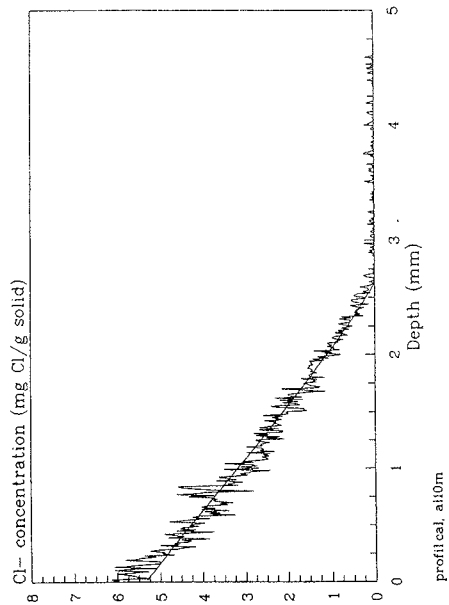
D=0.85E-12 m²/s



w/c=0.3, 0% sf, 30 days, 20°C

Anti-leach

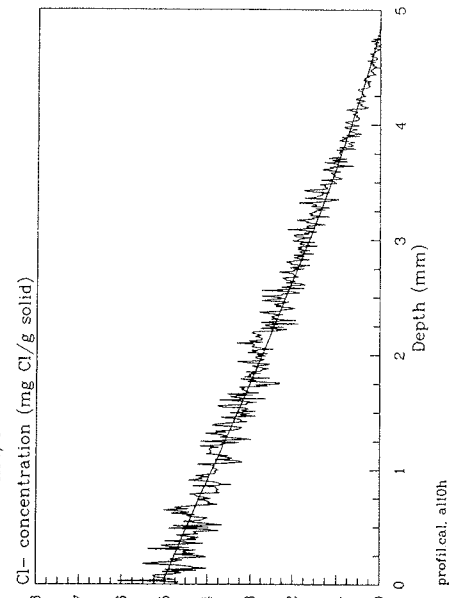
D=1.4E-12 m²/s



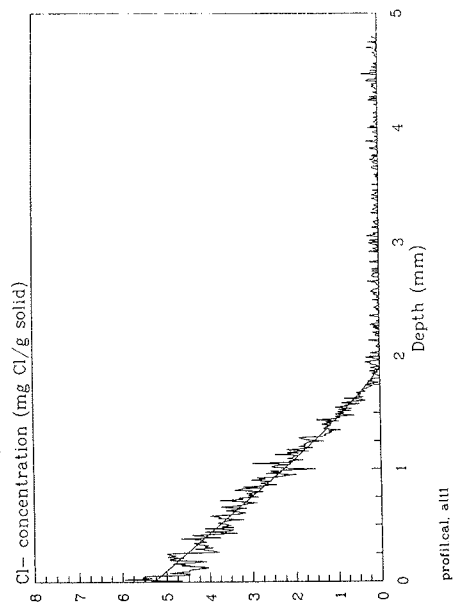
w/c=0.3, 0% sf, 30 days, 35°C

Anti-leach

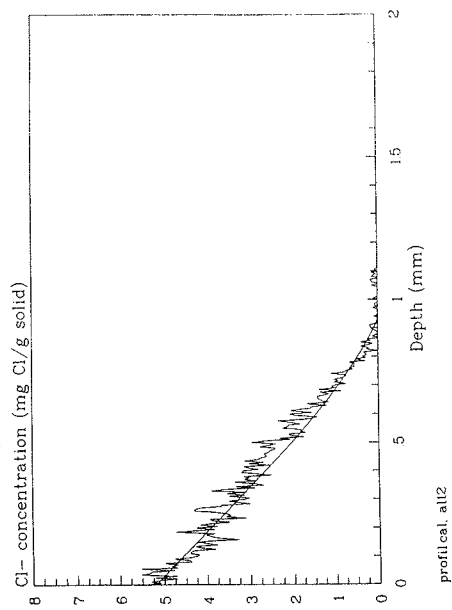
D=3.7E-12 m²/s



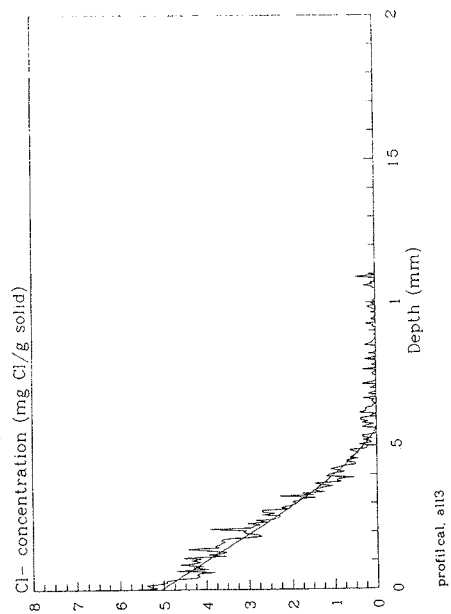
w/c=0.3, 3% sf, 30 days, 20°C
Anti-leach
D=0.7E-12 m²/s



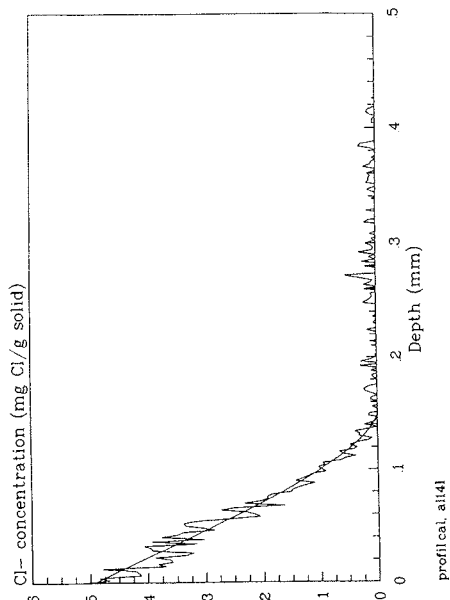
w/c=0.3, 6% sf, 30 days, 20°C
Anti-leach
D=0.15E-12 m²/s



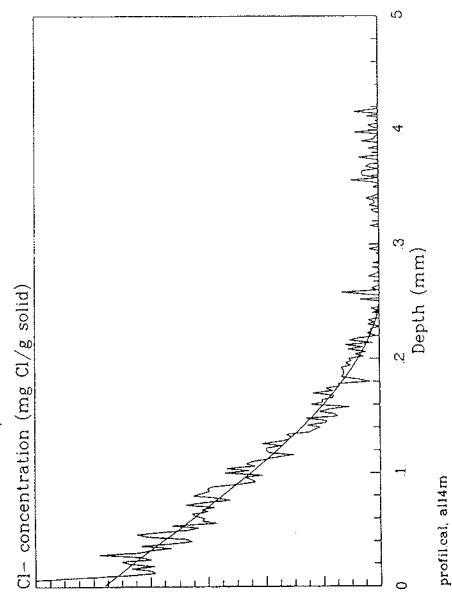
w/c=0.3, 10% sf, 30 days, 20°C
Anti-leach
D=0.050E-12 m²/s



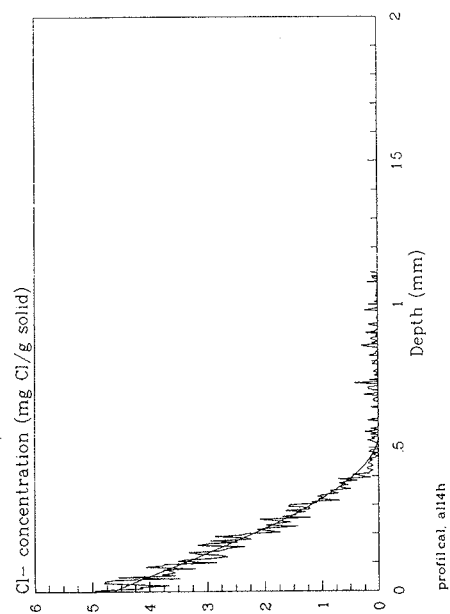
w/c=0.3, 20% sf, 30 days, 4°C
Anti-leach
D=0.004E-12 m²/s



w/c=0.3, 20% sf, 30 days, 20°C
Anti-leach
D=0.0080E-12 m²/s



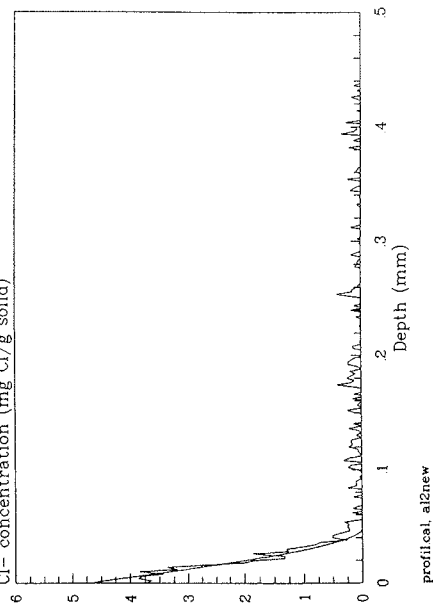
w/c=0.3, 20% sf, 30 days, 35°C
Anti-leach
D=0.028E-12 m²/s



w/c=0.3, 20% sf, 1 day, 20°C
Anti-leach

D=0.0080E-12 m²/s

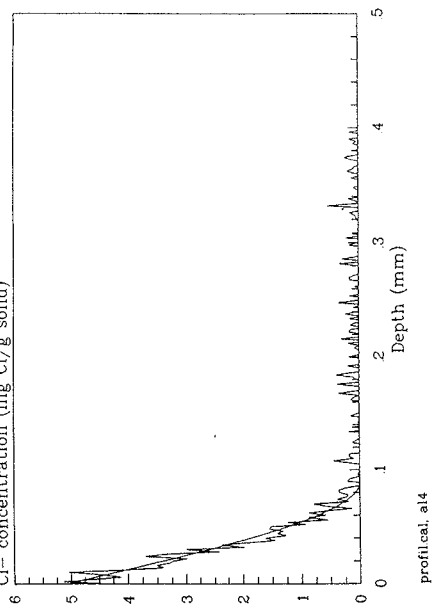
Cl⁻ concentration (mg Cl/g solid)



w/c=0.3, 20% sf, 3 days, 20°C
Anti-leach

D=0.0080E-12 m²/s

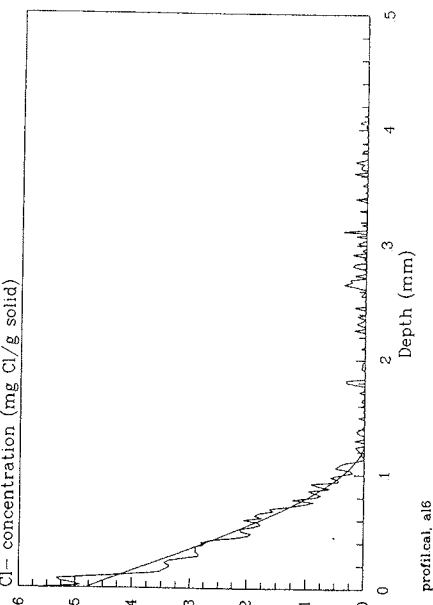
Cl⁻ concentration (mg Cl/g solid)



w/c=0.3, 20% sf, 7 days, 20°C
Anti-leach

D=0.0080E-12 m²/s

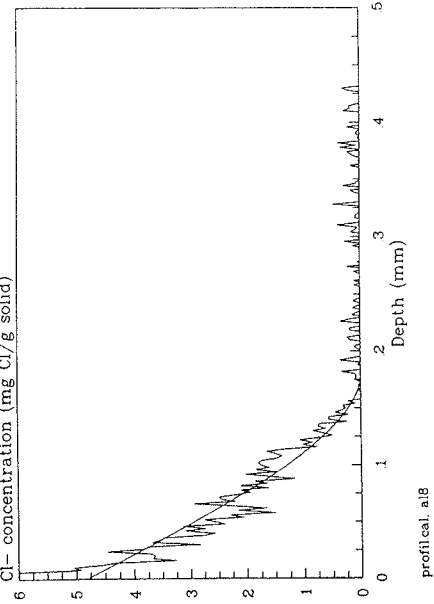
Cl⁻ concentration (mg Cl/g solid)



w/c=0.3, 20% sf, 14 days, 20°C
Anti-leach

D=0.0080E-12 m²/s

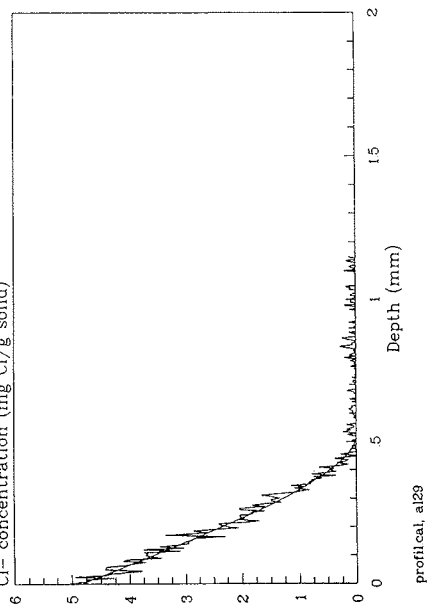
Cl⁻ concentration (mg Cl/g solid)



w/c=0.3, 20% sf, 90 days, 20°C
Anti-leach

D=0.012E-12 m²/s

Cl⁻ concentration (mg Cl/g solid)



LITERATURE

1. O. Mejlhede Jensen, Prefatory experiments - mixing recipe and procedure (in Danish), Ph.D. Thesis, Building Materials Laboratory, Technical University of Denmark, Technical Report 281/93, 1993
2. J. Skibsted, O.M. Jensen and H.J. Jakobsen, Hydration Kinetics for the Alite, Belite, and Calcium Aluminate Phase in Portland Cements from ^{27}Al and ^{29}Si MAS NMR Spectroscopy, 10th International Congress on The Chemistry of Cement, June 1997 (Göteborg), 2ii056
3. M.S.H. Korzen, Chloride binding in cement paste (in Danish), M.Sc. Thesis, Department of Structural Engineering and Materials, The Technical University of Denmark, March 1998
4. O. Mejlhede Jensen, Enclosures - measurements and notes (in Danish), Ph.D. Thesis, Building Materials Laboratory, Technical University of Denmark, Technical Report 285/93, 1993
5. R. McGregor, Diffusion and Sorption in Fibres and Films, Vol. 1, Academic Press, London, pp. 193-196, 1974
6. P.W. Atkins, Physical Chemistry, 3rd edition, Oxford University Press, Oxford, 1986
7. R. Parsons, Handbook of Electrochemical Constants, Butterworth, London, p. 79, 1959
8. R.C. Weast, CRC Handbook of Chemistry and Physics, 64th edition, CRC Press, Boca Raton, p. F-38, 1984
9. E.J. Garboczi, Modelling the electrical and diffusion properties of cement-based materials, Lecture No. 9, 7th ACBM/NIST computer modelling workshop, Washington, August 1996
10. L. Fuglsang Nielsen, Composite materials - mechanical and physical behaviour as influenced by phase geometry, Report (in press), Dep. of Structural Engineering and Materials, Technical University of Denmark, 1998
11. C.L. Page, N.R. Short and A. El Tarras, Diffusion of chloride ions in hardened cement pastes, Cement and Concrete Research, Vol. 11, pp. 395-406, 1981
12. T. Luping and L.-O. Nilsson, Chloride binding capacity and binding isotherms of OPC pastes and mortars, Cement and Concrete Research, Vol. 23, pp. 247-253, 1993
13. M. Collepardi, A. Marcialis and R. Turriziani, Penetration of Chloride Ions into Cement Pastes and Concretes, Journal of the American Ceramic Society, Vol. 55, No. 10, p. 534-535, 1972
14. C.M. Hansson, H. Strunge, J.B. Markussen and T. Frølund, The effect of cement type on the diffusion of chloride, Nordic Concrete Research, No. 4, 1985
15. S. Goto and D.M. Roy, Diffusion of ions through hardened cement pastes, Cement and Concrete Research, Vol. 11, pp. 751-757, 1981
16. Nordtest Standard, NT Build 443, Concrete, Hardened: accelerated chloride penetration, 1996
17. O.A. Kayyali and M.N. Haque, The Cl^-/OH^- ratio in chloride-contaminated concrete - a most important criterion, Magazine of Concrete Research, Vol 47, No. 172, Sept. pp. 235-242, 1995
18. J.M. Frederiksen, L.-O. Nilsson, E. Poulsen, P. Sandberg, H.E. Sørensen and O. Klinghoffer, HETEK, Chloride penetration into concrete State-of-the-Art, Transport processes, corrosion initiation, test methods and prediction models, "Final Draft", Report No. 53, The Danish Road Directorate, p. 118&123, 1996
19. O. Mejlhede Jensen, A.M. Coats and F.P. Glasser, Chloride ingress profiles measured by electron probe micro analysis, Cement and Concrete Research, Vol. 26, No. 11, pp. 1696-1705, 1996
20. R. Sørensen and M. Jansson, Chloride extraction from concrete, M.Sc. Thesis, Building Materials Laboratory, Technical University of Denmark, Technical Report 198/89, 1989
21. T. Luping, Chloride Transport in Concrete - measurement and prediction, Diss. Chalmers University of Technology, Department of Building Materials, Publication P-96:6, pp. 9-10, 1996
22. H.F.W Taylor, Cement chemistry, Academic press, pp. 403-404, 1991

23. B.F. Dela, Shrinkage cracks in high strength concrete (in Danish), Technical Report No. 333, M.Sc. Thesis, Building Materials Laboratory, Technical University of Denmark, 1995
24. A.W. Nienow, R. Unahabhokha and J.W. Mullin, Diffusion and mass transfer of ammonium and potassium chloride in aqueous solution, *Journal of applied Chemistry*, Vol. 18, May, pp. 154-156, 1968
25. V.T. Ngala and C.L. Page, Effects of carbonation on pore structure and diffusional properties of hydrated cement pastes, *Cement and Concrete Research*, Vol. 27 No. 7, pp. 995-1007, 1997
26. C.L. Page and P. Lambert, Kinetics of oxygen diffusion in hardened cement pastes, *Journal of Materials Science*, Vol. 22, pp. 942-946, 1987
27. E.L. Cussler, *Diffusion, Mass transfer in fluid systems*, Cambridge University Press, 1984
28. M. Mase, D. Colella, G. Radaelli and L. Bertolini, Simulation of chloride penetration in cement-based materials, *Cement and Concrete Research*, Vol. 27, No. 10, pp. 1591-1601, 1997
29. T.H. Wee, S.F. Wong, S. Swaddiwudhipong and S.L. Lee, A Prediction Method for Long-Term Chloride Concentration Profiles in Hardened Cement Matrix Materials, *ACI Materials Journal*, V. 94, No. 6, pp. 565-576, November-December 1997
30. A. Delagrave, J.P. Bigas, J.P. Ollivier, J. Marchand and M. Pigeon, Influence of the Interfacial Zone on the Chloride Diffusivity of Mortars, *Advanced Cement Based Materials*, No. 5, pp. 86-92, 1997
31. J. Crank, *The mathematics of diffusion*, 1. ed, Oxford University Press, London, 1964
32. H. Justnes, A review of chloride binding in cementitious systems, *Nordic Concrete Research*, Vol. 21, No. 1, pp. 48-63, 1998
33. R.K. Dhir, M.R. Jones and S.L.D. Ng, Prediction of total chloride content profile and concentration/time-dependent diffusion coefficients for concrete, *Magazine of Concrete Research*, Vol. 50, No. 1 March, pp. 37-49, 1998
34. E.J. Garboczi and D.P. Bentz, Chloride Diffusivity Computation for Cement Paste, Cement manufacture and use, *Proceedings of the Engineering Foundation Conference*, Potosi, Missouri, July 28-August 2, 1991
35. M. Nagesh and B. Bhattacharjee, Modeling of Chloride Diffusion in Concrete and Determination of Diffusion Coefficients, *ACI Materials Journal*, V. 95, No. 2, pp. 113-120, March-April 1998
36. H.G. Midgley and J.M. Illston, Effect of chloride penetration on the properties of hardened cement pastes, 7th international congress on the chemistry of cement, Vol. 3, pp. 101-103, VII, 1980
37. M.D.A. Thomas and C.M. Evans, Chloride penetration in high-performance concrete containing silica fume and fly ash, *Proceedings of the second international conference on Concrete under severe conditions*, Vol. 1, CONSEC'98 (ed. O.E. Gjrv, K. Sahai and N. Banthia), Troms, Norway, June 21-24, 1998, pp. 646-655, E&FN Spon, London 1998
38. S. Chatterji, Colloid Electrochemistry of Saturated Cement Paste and Some Properties of Cement Based Materials, *Advanced Cement Based Materials*, Vol. 7, No. 3/4, pp. 102-108, April/May 1998
39. H. Ushiyama and S. Goto, Diffusion of various ions in hardened portland cement paste, VI International congress on the chemistry of cement, Vol. 2 part 1, p. 331 Moscow, September, 1974
40. P. Lambert, C.L. Page and N.R. Short, Diffusion of chloride ions in hardened cement pastes containing pure cement minerals, *British Ceramic Proceedings*, Vol. 35, pp. 267-276, 1984
41. E.V. Srensen, Concrete with condensed silica fume. A preliminary study of strength and permeability (in Danish), Norwegian Institute of Technology, Trondheim, Report BML 82.610, pp. 189-202, 1982
42. E M Winkler, *Stone: Properties, Durability in Man's Environment*, Applied Mineralogy, 4, Springer-Verlag, p. 113-125, 1973
43. M. Collepardi, A. Marcialis and R. Turriziani, The kinetics of penetration of chloride ions into the concrete (in Italian), *Il cemento*, Vol. 67, No. 4, p. 157-164, 1970